Carbon-Aware Peer-to-Peer Joint Energy and Reserve Trading Market for Prosumers in Distribution Networks

Zehao Song, Yinliang Xu, *Senior Member, IEEE,* Lun Yang, and Hongbin Sun, *Fellow, IEEE*

***Abstract*—The increasing penetration of distributed energy resources (DERs) has facilitated the development of Peer-to-Peer (P2P) trading mechanism. An efficient P2P trading market framework is essential to integrate various kinds of DERs into new power systems while ensuring network security constraints (NSCs). This paper proposes a carbon-aware P2P trading market to realize joint energy and reserve trading for prosumers while satisfying NSCs of the distribution network (DN) simultaneously. A geometric series acceleration (GSA) method accelerated algorithm based on the consensus alternating direction method of multipliers (C-ADMM) is proposed to solve the distributed P2P trading problem. A data-driven method based on the two-sided distributionally robust chance constraint (TS-DRCC) is adopted to tackle with the uncertainty problem associated with DERs. Numerical tests on the IEEE 15-Bus distribution system and IEEE 141-Bus distribution system verify the advantages and effectiveness of the proposed method.**

***Index Terms*—Prosumers, carbon-aware, Peer-to-Peer, consensus alternating direction method of multipliers, geometric series acceleration method, distributionally robust chance constraint.**

NOMENCLATURE

A. Parameters

$P_{t,i,r}^{\mathbf{RES,fore}}$	RES r forecast power at time slot t.
φ^{RES}	System RES penetration level.
$a_{i,r}^{\mathbf{RES}}$	Curtailment cost coefficient of RES r.
$\underline{P}_{i,g}^{\mathbf{DG}}, \overline{P}_{i,g}^{\mathbf{DG}}$	Min/Max active power output of DG g.
$\underline{Q}_{i,g}^{\mathbf{DG}}, \overline{Q}_{i,g}^{\mathbf{DG}}$	Min/Max reactive power output of DG g.
$\Delta P_{i,g}^{\mathbf{DG}}, \lambda_{i,g}^{\mathbf{DG}}$	Ramping power/Power factor limit of DG g.
$a_{i,g}^{\mathbf{DG}}, b_{i,g}^{\mathbf{DG}}$	Generation csot coefficient of DG g.
$a_{i,g}^{\mathbf{DG,R}}$	Reserve cost coefficient of DG g.
$P_{t,i,m}^{\mathbf{L}}, Q_{t,i,m}^{\mathbf{L}}$	Active/Reactive power demand of load m.
$\overline{P}_{i}^{\mathbf{Grid}}, \overline{Q}_{i}^{\mathbf{Grid}}$	Maximum grid import active/reactive power.
$\overline{R}_{i}^{\mathbf{Grid,U}}, \overline{R}_{i}^{\mathbf{Grid,D}}$	Maximum grid import upward/downward reserve.
d_{ij}	Electrical distance between nodes i, j.
$\gamma^{\mathbf{E}}, \gamma^{\mathbf{Adj}}$	Network usage/Power adjustment cost coefficient.
$\pi_t^{\mathbf{E,P2P}}, \pi_t^{\mathbf{R,P2P}}$	P2P energy/reserve trading prices at time slot t.
$\pi_t^{\mathbf{E,Grid}}, \pi_t^{\mathbf{R,Grid}}$	Grid energy/reserve purchasing prices at time slot t.
$\widetilde{\pi}_t^{\mathbf{E,Grid}}, \widetilde{\pi}_t^{\mathbf{E,P2P}}$	Forecasted Grid/P2P energy purchasing prices at time slot t.
$\pi_t^{\mathbf{CER,Penalty}}$	CER penalty trading price at time slot t.
$\pi_t^{\mathbf{CER,P2P}}$	CER P2P trading price at time slot t.
$CER_{t,i}^{\mathbf{init}}$	Initial CER quantity at time slot t.
$e_t^{\mathbf{Grid}}$	Carbon emission factor of Grid at time slot t.
$e_{i,m}^{\mathbf{L}}, e_{i,g}^{\mathbf{DG}}$	Carbon emission factor of load/DG.
$e_{i,r}^{\mathbf{RES}}$	Carbon reduction reward factor of RES.
r_{ij}, x_{ij}	Branch resistance/reactance between nodes i, j.
$\underline{V}, \overline{V}$	Min/Max node voltage magnitude.
$\underline{P}_{ij}^{\mathbf{line}}, \overline{P}_{ij}^{\mathbf{line}}$	Min/Max branch active power limits.
$\underline{Q}_{ij}^{\mathbf{line}}, \overline{Q}_{ij}^{\mathbf{line}}$	Min/Max branch reactive power limits.
γ_t^M	Heavy ball acceleration coefficient at time slot t.
$\tau_{t,ij}^M, \omega_{t,ij}^M$	Self-adaptive penalty factor method parameters.
$\delta_M^{\mathrm{PE}}, \delta_M^{\mathrm{DE}}$	Primal/Dual residuals convergence criteria.
δ^{DN}	System residual convergence criteria.

Variables

$P_{t,i,r}^{\mathbf{RES}}, P_{t,i,r}^{\mathbf{RES,cut}}$	RES utilization/curtailment power at time slot t.
$R_{t,i,r}^{\mathbf{RES,D}}, R_{t,i,r}^{\mathbf{RES,U}}$	RES upward/downward reserve at time slot t.
q, z	Auxiliary variables for TS-DRCC problem.
$P_{t,i,g}^{\mathbf{DG}}, Q_{t,i,g}^{\mathbf{DG}}$	Active/Reactive power of DG g at time slot t.
$R_{t,i,g}^{\mathbf{DG,U}}, R_{t,i,g}^{\mathbf{DG,D}}$	Upward/Downward reserve of DG g at time slot t.
$CER_{t,i}^{\mathbf{Penalty}}$	CER penalty trading quantity at time slot t.
$CER_{t,i}^{\mathbf{P2P}}$	CER total P2P trading quantity at time slot

This work is supported by Shenzhen Science and Technology Program, Grant No. WDZC20231127152020001, National Natural Science Foundation of China, Grant No. 52277107 and Grant No. 52307138, and Tsinghua Shenzhen International Graduate School Interdisciplinary Research and Innovation Foundation, Grant No. JC2021004. *(Corresponding author: Yinliang Xu)*

Zehao Song and Yinliang Xu are with Tsinghua-Berkeley Shenzhen Institute, Tsinghua Shenzhen International Graduate School, Tsinghua University, Shenzhen, China (E-mail: songzh22@mails.tsinghua.edu.cn;xu.yinliang@sz.tsinghua.edu.cn).

L. Yang is with the System Engineering Institute, Xi'an Jiaotong University, Xi'an, China (Email: yanglun2019@gmail.com).

Hongbin Sun is with the Department of Electrical Engineering, Tsinghua University, Beijing, China (E-mail: shb@tsinghua.edu.cn).

t.

$P_{t,i}^{\mathbf{Grid}}, Q_{t,i}^{\mathbf{Grid}}$	Active/Reactive grid power at time slot t.
$R_{t,i}^{\mathbf{Grid,U}}, R_{t,i}^{\mathbf{Grid,D}}$	Upward/Downward grid reserve at time slot t.
$E_{t,ij}$	P2P energy trading quantity at time slot t.
$R_{t,ij}^{\mathbf{U}}, R_{t,ij}^{\mathbf{D}}$	P2P upward/downward reserve trading quantity at time slot t.
$P_{t,i}^{\mathbf{in}}, Q_{t,i}^{\mathbf{in}}$	Active/Reactive node injection power at time slot t.
$\Delta P_{t,j}^{\mathbf{in}}$	Node active power adjustment at time slot t.
$V_{t,j}$	Node voltage magnitude at time slot t.
$P_{t,ij}^{\mathbf{line}}, Q_{t,ij}^{\mathbf{line}}$	Active/Reactive branch power flow at time slot t.
$M_{t,ij}$	P2P M trading strategies at time slot t.
$\lambda_{t,ij}^{M}, \rho^{M}$	Dual variables/Penalty factor for P2P M trading.
$\mathbf{P}_{t}^{\mathbf{line}}, \mathbf{Q}_{t}^{\mathbf{line}}$	Active/Reactive power flow vectors at time slot t.
$\mathbf{V}_t$	Node voltage magnitude vector at time slot t.
$\Delta\mathbf{P}_{t}^{\mathbf{in}}$	Adjustment node power vector at time slot t.

I. Introduction

In the context of global warming and climate change, decarbonization has been regarded as an efficient and necessary way to mitigate environmental problems around the world. The energy sector accounts for nearly two-thirds of global greenhouse gas emissions [1] and thus needs revolutionary transformation. Fortunately, the declining investment and generation cost of renewable energy sources (RESs) enables the transition towards a renewable energy-dominated energy structure. However, the fundamental revolution in power systems brings great challenges as the penetration of distributed energy resources (DERs) like RESs and distributed generators (DGs) continues to grow [2]–[4]. Demand-side electricity users have changed their roles from conventional consumers to more proactive prosumers, who can both consume and produce power [5], [6]. Traditional top-down centralized operation structure [7] will be less efficient for new power systems with active prosumers. Efficient decentralized and distributed [8] operation mechanisms that can leverage the edge intelligence of individual prosumers are in an urgent need to fully exploit the operation flexibility potential of demand-side DERs [9].

Prosumers with different types of DERs have different operation characteristics, therefore, they will tend to make their own decisions according to their preferences. Peer-to-peer (P2P) mechanism [10] has emerged as a promising way to implement direct transactions between participants while respecting individual participants' preferences, interests, and information privacy. In this context, distributed optimization techniques have profound applications in P2P trading to implement prosumer-level decision-making processes.

The alternating direction method of multipliers (ADMM) method is a popular distributed optimization technique to solve the P2P trading problem. Different variants of the ADMM method have been developed to solve the distributed decision-making problem for individual prosumers. A Byzantine-resilient distributed P2P energy management method based on consensus ADMM (C-ADMM) is proposed in [11] to improve the resilience and efficiency of the P2P mechanism against untruthful information disturbance. In [12], a scalable P2P energy trading mechanism based on fast ADMM (F-ADMM) using a closed-form solution is proposed to establish a prosumer-centric transactive energy market. A robust ADMM algorithm fighting against communication failures is proposed in [13] to implement P2P energy trading in an unbalanced distribution network (DN). To further preserve prosumers' heterogeneous (source of generation and financial benefit, etc.) preferences, a P2P energy market based on multi-class energy management is proposed in [14] and implemented by the ADMM method. In [15], the ADMM technique is used to decompose centralized P2P energy and ancillary service trading market clearing process. A network-constrained P2P energy trading method for multiple microgrids (MGs) considering uncertainty is proposed in [16]. Scenario-based stochastic optimization (SO) is adopted to handle with the uncertainty of DERs in MG. Based on the end-edge-cloud structure, a communication-censored ADMM method is proposed to implement P2P energy trading among community users in [17]. From the above-mentioned literatures, we can find that most existing researches only investigate the energy trading problem for prosumers. Few researchers have studied the reserve trading problems associated with the uncertainties of DERs and the carbon emission obligation problem among electricity demand-side and generation-side stakeholders. Yet these two critical problems will be crucial for the future power system with increasing penetration of DERs, which motivate this work.

Due to the inherent stochastic and fluctuating characteristics of RES, the uncertainty problem that comes along with high penetration RES will bring great challenges to the safe and stable operation of the power system. Therefore, maintaining reserve capacity is vital to ensure the system's operation security. Traditionally, the distribution network operator (DNO) will determine system-wide reserve capacity by empirical knowledge or some optimization techniques like robust optimization (RO) [18]. This kind of centralized decision approach may not be suitable for new power systems with prosumers. On the one hand, increasing the penetration of RES will inevitably increase the reserve capacity burden of DNO. On the other hand, prosumers with RESs should be responsible for their power deviation when participating in the P2P trading market. Therefore, it will be better to let individual prosumers evaluate their reserve capacity requirements by themselves and participate in the reserve market to negotiate P2P reserve transactions with other prosumers.

Recent advanced researches have made great effort to investigate the joint energy and reserve scheduling mechanism. A bi-level SO model is proposed in [19] to implement P2P energy and reserve trading between wind power producers (WPP) and demand response aggregators (DRAs) based on bilateral contracts. In [20], the reserve capacity requirements of individual prosumers are determined by the chance-

constrained (CC) method considering versatile distribution.

The above-mentioned SO and CC methods rely on exact uncertainty sample or probability distribution function (PDF), which is hard to obtain in the real-world application. How to properly determine reasonable reserve capacity is still an open question. Currently, distributionally robust optimization (DRO) has profound applications in power system operation considering uncertainty for its robustness against inaccuracy of the predicted PDF of the uncertainty. In [21], a Wasserstein metric (WM) based DRO method is developed to take uncertainties from RES and user load consumption into consideration. Yet the reserve scheduling problem in [21] is still designed for MG-level operators, i.e., the reserve scheduling of DGs and energy storage systems (ESSs) inside MG is still performing in a centralized manner. Some recent researches have investigated the prosumer-level reserve determination and scheduling problem. A joint P2P energy and reserve sharing mechanism considering uncertainty and limited communication resources is proposed in [22]. However, network security constraints (NSCs) like line power flow constraints and node voltage magnitude constraints are not taken into consideration in [22] and thus the proposed method may lead to NSCs violations in distribution-level power systems. To overcome the above-mentioned research gaps, a prosumer-level reserve determination method that doesn't rely on the exact knowledge of the uncertainty is imperative to accommodate more DERs. Furthermore, the NSCs are not neglectable in practical distribution-level P2P trading applications.

Motivated by the goal of decarbonization, many researchers have made great efforts to investigate power system low-carbon operation. It should be emphasized that demand-side electricity user is the true underlying factor that causes carbon emission in power systems rather than generation-side generators [23]. In this context, the carbon trading mechanism has emerged as a promising way to encourage low-carbon energy utilization in future power systems. A P2P joint energy and carbon trading mechanism based on the decomposable carbon-aware distribution locational marginal pricing (CDLMP) is proposed in [24] to promote both economic, secure and low-carbon operation of DN. A distributed energy and carbon emission rights (CERs) trading mechanism considering demand-side carbon emission obligation is implemented by C-ADMM in [25]. To implement cost-efficient decarbonization, a risk-averse stochastic P2P joint energy and carbon emission allowance trading market is proposed in [26] based on Stackelberg game theory. The above-mentioned researches have investigated the energy-carbon nexus in the P2P energy and carbon trading market. Yet the joint energy, reserve, and carbon (E&R&C) trading market for prosumers has not been sufficiently investigated to further promote the prosumers' low-carbon power utilization while enhancing the power network operation security.

Inspired by the aforementioned pioneering works, a carbon-aware P2P joint energy and reserve trading market for prosumers considering NSCs and uncertainty is proposed. The comparison with the state-of-art works is shown in Table I. The main contributions of this paper are listed as follows.

- The co-optimization of energy and reserve trading and carbon trading is implemented in the proposed P2P joint E&R&C trading market. Compared with the electricity and carbon (E&C) trading market which doesn't consider the uncertainties of DERs proposed in previous researches [24], [25], the proposed P2P joint E&R&C trading market can further promote low-carbon power utilization while enhancing system operation security.
- Unlike the SO/CC-based centralized reserve determination methods in [19], [20] and WM-DRO-based MG-level reserve determination method in [21], a data-driven prosumer-level reserve determination method based on the two-sided distributionally robust chance constraint (TS-DRCC) is proposed in this paper, which can both enhance the fairness of reserve allocation and reduce dependency on accurate knowledge of the uncertainty.
- An accelerated C-ADMM algorithm based on the geometric series acceleration (GSA) method with fully distributed self-adaptive penalty factors is proposed for the first time. Compared to the existing heavy ball acceleration-based and Nesterov acceleration-based distributed algorithms [27], [28], the proposed algorithm can achieve better operation efficiency and accuracy during the P2P trading market operation process.

TABLE I
COMPARISON WITH THE STATE-OF-ART WORKS

Reference	Prosumer-level reserve scheduling	Network constraints	Joint E&R&C trading	Network usage charge
[16], [21], [25]	–	Yes	–	–
[11]–[15], [24]	–	Yes	–	Yes
[22]	Yes (WM-DRO)	–	–	–
This paper	Yes (TS-DRCC)	Yes	Yes	Yes

* Yes: The item is considered. -: The item is not considered.

The rest of the paper is organized as follows: Section II demonstrates the proposed prosumer-level reserve determination method. Section III presents the framework of the proposed P2P joint E&R&C trading market. The detailed implementation process is shown in Section IV. Section V provides numerical tests with the IEEE 15-Bus distribution system and the IEEE 141-Bus distribution system. Section VI concludes this paper.

II. PROSUMER-LEVEL RESERVE DETERMINATION

Prosumers equipped with RESs need to determine their upward/downward reserve capacity requirements before participating in the P2P joint E&R&C trading market.

The ambiguity set describing the uncertain RES power forecast error distribution $\mathbb{P}_{\xi_t}$ at time slot t is formulated based on mean and covariance information as follows:

$$\mathcal{P} := \{\mathbb{P}_{\xi_t} : \mathbb{E}_{\mathbb{P}}[\xi_t] = \mu, \mathbb{E}_{\mathbb{P}}[(\xi_{\mathbf{t}} - \mu)(\xi_{\mathbf{t}} - \mu)^\top] = \mathbf{\Sigma}\} \quad (1)$$

where $\mathbb{E}_{\mathbb{P}}$ denotes the expectation operator and ξ_t is the RES forecast error at time slot t, μ and $\mathbf{\Sigma}$ are mean value vector and covariance matrix of ξ_t, respectively.

The upward/downward reserve requirements of a prosumer equipped with RES located at node i are defined as follows:

$$\xi_t = \xi_t^+ - \xi_t^- \quad (2a)$$

$$e_i[n] = \begin{cases} 0, n \neq i \\ 1, n = i \end{cases} \quad (2b)$$

$$R_{t,i,r}^{\mathrm{RES,U}} = {e_i}^\top \xi_t^-, R_{t,i,r}^{\mathrm{RES,D}} = {e_i}^\top \xi_t^+ \quad (2c)$$

where (2a) means that the RES generation power deviation can be divided into two parts including upward/downward deviation denoting increase/decrease power output of RES, respectively. (2b) defines the RES indicator vector of size $(\mathcal{N}^{\mathcal{B}} \times 1)$ for prosumer located at node i, $\mathcal{N}^{\mathcal{B}}$ is the number of system nodes and $e_i[n]$ is the nth element of e_i. (2c) contains the upward/downward reserve requirements defined as $R^{\mathrm{RES,U}}_{t,i,r}$ / $R^{\mathrm{RES,D}}_{t,i,r}$ at time slot t.

The reserve determination problem based on TS-DRCC for individual prosumer located at node i is formulated as follows:

$$\min \sum_{r} (R^{\mathrm{RES,D}}_{t,i,r} + R^{\mathrm{RES,U}}_{t,i,r}) \tag{3a}$$

$$s.t. \inf_{\mathbb{P}_{\xi_t} \in \mathcal{P}} \mathbb{P}_{\xi_t}[-R^{\mathrm{RES,U}}_{t,i,r} \leqslant {e_i}^{\top} \xi_t \leqslant R^{\mathrm{RES,D}}_{t,i,r}] \geqslant 1 - \varepsilon_i \tag{3b}$$

where ε_i is the risk preference parameter of the prosumer located at node i describing the probability of not satisfying the reserve requirement constraint. This paper assumes that every prosumer can determine its reserve requirements according to its risk preference parameter, thus individual chance constraint is imposed on each prosumer. The proposed prosumer-level reserve determination method is consistent with practical P2P trading application situations, every prosumer determines its trading requirements by its preference without knowing other prosumer's preference.

The origin problem is intractable due to inexact constraint (3b). We can rewrite (3b) as a generic symmetrical TS-DRCC given as follows:

$$\inf_{\mathbb{P}_{\xi_t} \in \mathcal{P}} \mathbb{P}_{\xi_t}[-T_1(x^{\mathrm{RES,R}}_{t,i,r}) \leqslant {e_i}^{\top} \xi_t - T_2(x^{\mathrm{RES,R}}_{t,i,r}) \leqslant T_1(x^{\mathrm{RES,R}}_{t,i,r})] \geqslant 1 - \varepsilon_i \tag{4a}$$

$$x^{\mathrm{RES,R}}_{t,i,r} = \{R^{\mathrm{RES,D}}_{t,i,r}, R^{\mathrm{RES,U}}_{t,i,r}\} \tag{4b}$$

$$T_1(x^{\mathrm{RES,R}}_{t,i,r}) = \frac{R^{\mathrm{RES,D}}_{t,i,r} + R^{\mathrm{RES,U}}_{t,i,r}}{2}, T_2(x^{\mathrm{RES,R}}_{t,i,r}) = \frac{R^{\mathrm{RES,D}}_{t,i,r} - R^{\mathrm{RES,U}}_{t,i,r}}{2} \tag{4c}$$

Following [29], the origin intractable problem can be reformulated as a tractable second-order cone (SOC) form as follows:

$$\min \sum_{r} (R^{\mathrm{RES,D}}_{t,i,r} + R^{\mathrm{RES,U}}_{t,i,r}) \tag{5a}$$

$$s.t. \left\{ \begin{array}{c} q^2 + {e_i}^{\top} \mathbf{\Sigma} e_i \leq \varepsilon_i \Big(T_1(x^{\mathrm{RES,R}}_{t,i,r}) - z \Big)^2 \\ -(q+z) \leq -T_2(x^{\mathrm{RES,R}}_{t,i,r}) \leq (q+z) \\ 0 \leq z \leq T_1(x^{\mathrm{RES,R}}_{t,i,r}), 0 \leq q \end{array} \right\} \tag{5b}$$

The reserve determination method for the uncertainty of load is consistent with that of RES mentioned above. For the clarity of the paper, the detailed uncertainty modeling and reserve determination are given in Appendix-A.

III. P2P JOINT E&R&C TRADING MARKET

The main framework of the proposed P2P joint E&R&C trading market is shown in Fig. 1. As the P2P transaction framework shows, prosumers with load demand can purchase energy from other prosumers with DG and RES. Prosumers equipped with RES can purchase reserve power from prosumers equipped with DG to satisfy part of their reserve capacity requirements. Particularly, the P2P CER trading between prosumers is considered in this framework to promote low-carbon power utilization. Carbon emission obligation is considered on both demand-side and generation-side in this work. Prosumers need to compensate for their load power consumption as well as the high carbon emission power generation of DGs by purchasing CERs. In contrast, prosumers providing clean power generation of RESs will be rewarded with extra CERs and can get profits by selling CERs in the P2P CER trading market. To further motivate prosumers to reduce carbon emission, CER penalty costs will be allocated to prosumers who can not compensate for their CER requirements by participating in the P2P CER trading market.

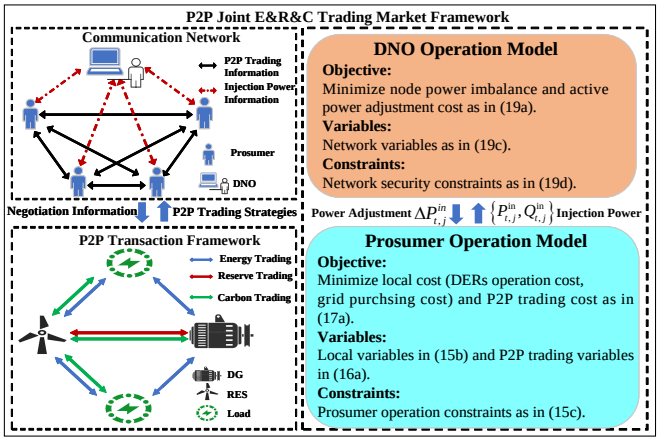

Fig. 1. P2P joint E&R&C trading market framework.

The system information exchange process is shown in the communication network, prosumers can directly negotiate with their P2P trading partners and only need to submit node injection power information to DNO for system operation security concerns. After receiving the node injection power information from prosumers, the DNO will check whether the P2P transactions between prosumers in the physical network will violate NSCs or not. Necessary node injection power adjustments will be allocated to corresponding prosumers to ensure system operation security.

A. Preliminary

We consider a radial DN connecting prosumers at different nodes, which can be demoted as an undirected graph $\mathcal{G}(\mathcal{N}^{\mathcal{B}}, \mathcal{N}^{\mathcal{L}})$ in this work. The graph consists of a set of nodes $\mathcal{N}^{\mathcal{B}} := [1, ..., N]$ indexed by i, j and a set of branches $\mathcal{N}^{\mathcal{L}} := [l \rightarrow (i,j)] \subseteq \mathcal{N}^{\mathcal{B}} \times \mathcal{N}^{\mathcal{B}}$ indexed by l. Note that each prosumer owns several DERs. The RES, DG and load of the prosumer connected to bus i are indexed by r, g, m, respectively.

B. DER Operation Constraints

i) RES Operation Constraints: Constraints (6a)-(6b) are RES operation constraints. (6a) limits the maximum power output of RES while (6b) defines the RES curtailment power. We consider the RES curtailment penalty costs for prosumers equipped with RES. Note that the costs of the prosumers equipped with RES for purchasing upward/downward reserve will be cleared in the reserve trading market.

$$0 \leqslant P^{\mathrm{RES}}_{t,i,r} \leqslant P^{\mathrm{RES,fore}}_{t,i,r} \tag{6a}$$

$$P_{t,i,r}^{\text{RES,cut}} = P_{t,i,r}^{\text{RES,fore}} - P_{t,i,r}^{\text{RES}} \tag{6b}$$

$$C_{t,i,r}^{\text{RES,cut}}(P_{t,i,r}^{\text{RES,cut}}) = a_{i,r}^{\text{RES}} P_{t,i,r}^{\text{RES,cut}} \tag{6c}$$

ii) DG Operation Constraints: Constraints (7a)-(7e) are DG operation constraints. (7a) ensures that the DG generation power plus the upward reserve will not exceed the upper bound of DG active power output. (7b) ensures that the DG generation power minus the downward reserve will not exceed the lower bound of DG active power output. (7c) limits the ramping active power of DG. Since the P2P trading market is operated sequentially, the participants can only make decisions according to the current or past information. The active power generation decision variable determined at the last time period $P_{t-1,i,g}$ is a known parameter during the prosumer's decision process at the current time period. (7d) limits the reactive power output of DG. (7e) ensures the power factor of DG maintains within pre-defined limits. Note that the revenue of the prosumers equipped with DG for providing upward/downward reserve will be cleared in the reserve trading market.

$$P_{t,i,g}^{\text{DG}} + R_{t,i,g}^{\text{DG,U}} \leqslant \overline{P}_{i,g}^{\text{DG}} \tag{7a}$$

$$\underline{P}_{i,g}^{\text{DG}} \leqslant P_{t,i,g}^{\text{DG}} - R_{t,i,g}^{\text{DG,D}} \tag{7b}$$

$$P_{t-1,i,g}^{\text{DG}} - \Delta P_{i,g}^{\text{DG}} \leq P_{t,i,g}^{\text{DG}} \leq P_{t-1,i,g}^{\text{DG}} + \Delta P_{i,g}^{\text{DG}} \tag{7c}$$

$$\underline{Q}_{i,g}^{\text{DG}} \leqslant Q_{t,i,g}^{\text{DG}} \leqslant \overline{Q}_{i,g}^{\text{DG}} \tag{7d}$$

$$tan(cos^{-1}(-\lambda_{i,g}^{\text{DG}})) \leqslant \frac{Q_{t,i,g}^{\text{DG}}}{P_{t,i,g}^{\text{DG}}} \leqslant tan(cos^{-1}(\lambda_{i,g}^{\text{DG}})) \tag{7e}$$

$$\begin{aligned} C_{t,i,g}^{\text{DG}}(P_{t,i,g}^{\text{DG}}, R_{t,i,g}^{\text{DG,U}}, R_{t,i,g}^{\text{DG,D}}) &= a_{i,g}^{\text{DG}}(P_{t,i,g}^{\text{DG}})^2 + b_{i,g}^{\text{DG}} P_{t,i,g}^{\text{DG}} \\ &+ a_{i,g}^{\text{DG,R}}(R_{t,i,g}^{\text{DG,U}} + R_{t,i,g}^{\text{DG,D}}) \end{aligned} \tag{7f}$$

C. Energy and Reserve Trading Market

The active/reactive power balance constraints of individual prosumer located at node i are described by (8a)-(8b) while the upward/downward balance constraints of individual prosumer located at node i are described by (8c)-(8d). The constraint for imported active/reactive power from the grid of individual prosumer located at node i is described by (8e). The constraint for imported upward/downward reserve from the grid of individual prosumer located at node i is described by (8f).

$$P_{t,i}^{\text{Grid}} + \sum_{g} P_{t,i,g}^{\text{DG}} + \sum_{r} P_{t,i,r}^{\text{RES}} + \sum_{j \in \omega_i} E_{t,ij} = \sum_{m} P_{t,i,m}^{\text{L}} \tag{8a}$$

$$Q_{t,i}^{\text{Grid}} + \sum_{g} Q_{t,i,g}^{\text{DG}} = \sum_{g} Q_{t,i,m}^{\text{L}} \tag{8b}$$

$$R_{t,i}^{\text{Grid,U}} + \sum_{g} R_{t,i,g}^{\text{DG,U}} + \sum_{j \in \omega_i}^{m} R_{t,ij}^{\text{U}} = \sum_{r}^{m} R_{t,i,r}^{\text{RES,U}} + \sum_{m} R_{t,i,m}^{\text{Load,U}} \tag{8c}$$

$$R_{t,i}^{\text{Grid,D}} + \sum_{g} R_{t,i,g}^{\text{DG,D}} + \sum_{j \in \omega_i} R_{t,ij}^{\text{D}} = \sum_{r} R_{t,i,r}^{\text{RES,D}} + \sum_{m} R_{t,i,m}^{\text{Load,D}} \tag{8d}$$

$$0 \leqslant P_{t,i}^{\text{Grid}} \leqslant \overline{P}_{i}^{\text{Grid}}, 0 \leqslant Q_{t,i}^{\text{Grid}} \leqslant \overline{Q}_{i}^{\text{Grid}} \tag{8e}$$

$$0 \leqslant R_{t,i}^{\text{Grid,U}} \leqslant \overline{R}_{i}^{\text{Grid,U}}, 0 \leqslant R_{t,i}^{\text{Grid,D}} \leqslant \overline{R}_{i}^{\text{Grid,D}} \tag{8f}$$

The total P2P energy and upward/downward reserve trading quantity of individual prosumer located at node i is described by (9a) while the P2P trading balance constraint is ensured by (9b).

$$E_{t,i} = \sum_{j \in \omega_i} E_{t,ij}, R_{t,i}^{\text{U}} = \sum_{j \in \omega_i} R_{t,ij}^{\text{U}}, R_{t,i}^{\text{D}} = \sum_{j \in \omega_i} R_{t,ij}^{\text{D}} \tag{9a}$$

$$E_{t,ij} + E_{t,ji} = 0, R_{t,ij}^{\text{U}} + R_{t,ji}^{\text{U}} = 0, R_{t,ij}^{\text{D}} + R_{t,ji}^{\text{D}} = 0 \tag{9b}$$

To take the network impact of the prosumers' P2P transactions into consideration to realize grid-friendly P2P trading, the network usage fee is defined as follows:

$$d_{ij} = \sum_{l \in \Pi_{ij}} |z_l| \tag{10a}$$

$$u_{t,ij}(E_{t,ij}) = \gamma^{\text{E}} d_{ij} (E_{t,ij})^2 \tag{10b}$$

where (10a) defines the electrical distance as aggregated impedances of the connected branches between prosumers located at nodes i and j. Note that d_{ij} is unique in radial DN and can be determined by using the shortest path algorithms [30]. Π_{ij} is the set of branches connecting nodes i and j. z_l is the impedance of branch l. (10b) defines the network usage fee for delivering P2P energy transactions between prosumer located at nodes i and j.

Based on the above constraints and definitions, the cost functions for the individual prosumer participating in the energy and reserve trading market can be defined as follows:

$$C_{t,i}^{\text{E}}(E_{t,i}) = \sum_{j \in \omega_i} \pi_t^{\text{E,P2P}} E_{t,ij} \tag{11a}$$

$$C_{t,i}^{network}(E_{t,i}) = \frac{1}{2} \sum_{j \in \omega_i} u_{t,ij}(E_{t,ij}) \tag{11b}$$

$$C_{t,i}^{\text{R}}(R_{t,i}^{\text{U}}, R_{t,i}^{\text{D}}) = \sum_{j \in \omega_i} \pi_t^{\text{R,P2P}}(R_{t,i}^{\text{U}} + R_{t,i}^{\text{D}}) \tag{11c}$$

where (11a) is the P2P energy trading cost function and (11b) is the network usage cost function of P2P energy transactions. (11c) is the P2P reserve trading cost function. ω_i is the set of P2P trading partners of the prosumer located at node i.

The cost functions for individual prosumer to import energy and reserve from the grid can be defined as follows:

$$C_{t,i}^{\text{E,Grid}}(P_{t,i}^{\text{Grid}}) = \pi_t^{\text{E,Grid}} P_{t,i}^{\text{Grid}} \tag{12a}$$

$$C_{t,i}^{\text{R,Grid}}(R_{t,i}^{\text{Grid,U}}, R_{t,i}^{\text{Grid,D}}) = \pi_t^{\text{R,Grid}}(R_{t,i}^{\text{Grid,U}} + R_{t,i}^{\text{Grid,D}}) \tag{12b}$$

where (12a) is the cost function of the prosumer purchasing power from the grid and (12b) is the cost function of the prosumer purchasing upward/downward reserve from the grid, respectively. Note that according to the mid-market rate (MMR) pricing scheme which is widely adopted in state-of-art P2P trading market as in [31], [32], the P2P energy trading price $\pi_t^{\text{E,P2P}}$ is set to be lower than the upstream electricity price $\pi_t^{\text{E,Grid}}$. The MMR pricing scheme is also applied in the P2P reserve trading in this work. This kind of market pricing scheme aims to promote P2P trading among prosumers. When prosumers need to purchase energy/reserve, since the purchasing price from the upstream grid is higher than the P2P trading price under the MMR pricing scheme, they will tend to purchase energy/reserve from other prosumers

as their first choice. Moreover, since the feed-in tariff is set to be lower than that of the P2P trading price under the MMR pricing scheme, the prosumers will also tend to sell their surplus energy/reserve to other prosumers in need to get more profits. When the upstream electricity price changes, the prosumers will tend to decrease the utilization of power supply with higher cost and increase the utilization of power supply with lower cost. In accordance with state-of-art P2P trading researches [32]–[34] using MMR pricing mechanism, this paper focuses on designing an efficient P2P trading mechanism among prosumers and thus the uncertainty of upstream electricity price is not the main research objective of this work. The impact of the uncertainty of upstream electricity price is elaborated in Section V-B4 in detail.

D. CER Trading Market

The CER trading market operation constraints are described by (13a)-(13e). (13a) is the CER balance constraint for each prosumer. In accordance with [25] and [33], the initial CER allocation process is based on the historical data of the prosumer's load power, e.g., the $CER_{t,i}^{\text{init}}$ is proportional to the historical load power of the prosumer connected to bus i. The total P2P CER trading quantity is described by (13b) while the P2P CER trading balance constraint is described by (13c). (13d) ensures that the CER penalty term is non-negative. (13e) can be interpreted from the following two aspects: 1) If the prosumer needs to purchase CER in the market, then its total CER P2P trading quantity is non-negative (purchase CER from other prosumers). Therefore, the production of two non-negative items is still non-negative. Then (13e) holds. 2) If the prosumer sells CER in the market, then its total CER P2P trading quantity is negative (sell CER to other prosumers). It means that its CER penalty term is zero. Then, the production of its total CER P2P trading quantity and its CER penalty term is zero. Therefore, (13e) still holds.

$$CER_{t,i}^{\text{init}} + CER_{t,i}^{\text{Penalty}} + CER_{t,i}^{\text{P2P,Total}} = e_t^{\text{Grid}} P_{t,i}^{\text{Grid}} + \sum_m e_{i,m}^{\text{L}} P_{t,i,m}^{\text{L}} + \sum_g e_{i,g}^{\text{DG}} P_{t,i,g}^{\text{DG}} - \sum_r e_{i,r}^{\text{RES}} P_{t,i,r}^{\text{RES}} \tag{13a}$$

$$CER_{t,i}^{\text{P2P,Total}} = \sum_{j \in \omega_i} CER_{t,ij}^{\text{P2P}} \tag{13b}$$

$$CER_{t,ij}^{\text{P2P}} + CER_{t,ji}^{\text{P2P}} = 0 \tag{13c}$$

$$CER_{t,i}^{\text{Penalty}} \geqslant 0 \tag{13d}$$

$$CER_{t,i}^{\text{P2P,Total}} \cdot CER_{t,i}^{\text{Penalty}} \geq 0 \tag{13e}$$

The P2P CER trading cost function is defined as (14).

$$\begin{aligned} &C_{t,i}^{\text{CER}}(CER_{t,i}^{\text{Penalty}}, CER_{t,i}^{\text{P2P,Total}}) \\ &= \pi_t^{\text{CER,Penalty}} CER_{t,i}^{\text{Penalty}} + \pi_t^{\text{CER,P2P}} CER_{t,i}^{\text{P2P,Total}} \end{aligned} \tag{14}$$

IV. DISTRIBUTED IMPLEMENTATION OF P2P TRADING MARKET UNDER DISTRIBUTION NETWORK CONSTRAINTS

We can formulate prosumer's objective function when participating the joint E&R&C trading market as follows:

$$\begin{aligned} C_{t,i}^{\text{pro}}(x_{t,i}^{\text{pro}}) = &\underbrace{\sum_r C_{t,i,r}^{\text{RES,cut}}(P_{t,i,r}^{\text{RES,cut}}) + \sum_g C_{t,i,g}^{\text{DG}}(P_{t,i,g}^{\text{DG}}, R_{t,i,g}^{\text{DG,U}}, R_{t,i,g}^{\text{DG,D}})}_{\text{DER operation cost}} \\ &+ \underbrace{C_{t,i}^{\text{E,Grid}}(P_{t,i}^{\text{Grid}})}_{\text{Grid Energy trading cost}} + \underbrace{C_{t,i}^{\text{R,Grid}}(R_{t,i}^{\text{Grid,U}}, R_{t,i}^{\text{Grid,D}})}_{\text{Grid Reserve trading cost}} \\ &+ \underbrace{C_{t,i}^{\text{E}}(E_{t,i}) + C_{t,i}^{network}(E_{t,i})}_{\text{P2P Energy trading cost}} + \underbrace{C_{t,i}^{\text{R}}(R_{t,i}^{\text{U}}, R_{t,i}^{\text{D}})}_{\text{P2P Reserve trading cost}} \\ &+ \underbrace{C_{t,i}^{\text{CER}}(CER_{t,i}^{\text{Penalty}}, CER_{t,i}^{\text{P2P,Total}})}_{\text{P2P CER trading cost}} \end{aligned} \tag{15a}$$

$$x_{t,i}^{\text{pro}} := \left\{ \begin{array}{c} \underbrace{P_{t,i,r}^{\text{RES,cut}}, P_{t,i,g}^{\text{DG}}, Q_{t,i,g}^{\text{DG}}, R_{t,i,g}^{\text{DG,U}}, R_{t,i,g}^{\text{DG,D}}}_{\text{DER Operation Strategies}} \\ \underbrace{P_{t,i}^{\text{Grid}}, Q_{t,i}^{\text{Grid}}, R_{t,i}^{\text{Grid,U}}, R_{t,i}^{\text{Grid,D}}}_{\text{Grid Import Strategies}} \\ \underbrace{E_{t,i}, R_{t,i}^{\text{U}}, R_{t,i}^{\text{D}}}_{\text{P2P Energy \& Reserve Trading Strategies}} \\ \underbrace{CER_{t,i}^{\text{Penalty}}, CER_{t,i}^{\text{P2P,Total}}}_{\text{P2P Carbon Trading Strategies}} \end{array} \right\} \tag{15b}$$

$$s.t. \left\{ \begin{array}{l} \textbf{RES Constraints: } (6a)-(6b). \\ \textbf{DG Constraints: } (7a)-(7e). \\ \textbf{Energy and Reserve Constraints: } \\ (8a)-(8f), (9a)-(9b). \\ \textbf{Carbon Constraints: } (13a)-(13e). \end{array} \right\} \tag{15c}$$

The compact form of the prosumers' P2P trading strategies, dual variables and penalty factors are listed as follows:

$$M_{t,ij}^k = \left\{ E_{t,ij}^k, R_{t,ij}^{\text{U},k}, R_{t,ij}^{\text{D},k}, CER_{t,ij}^{\text{P2P},k} \right\} \tag{16a}$$

$$\lambda_{t,ij}^{M,k} = \left\{ \lambda_{t,ij}^{\text{E},k}, \lambda_{t,ij}^{\text{R,U},k}, \lambda_{t,ij}^{\text{R,D},k}, \lambda_{t,ij}^{\text{CER},k} \right\} \tag{16b}$$

$$\rho^{M,k} = \left\{ \rho^{\text{E},k}, \rho^{\text{R,U},k}, \rho^{\text{R,D},k}, \rho^{\text{CER},k} \right\} \tag{16c}$$

where (16a) is the compact form of the prosumers' joint E&R&C trading strategies(primal variables), (16b) is the compact form of the prosumers' joint E&R&C trading dual variables and (16c) is the compact form of the prosumers' penalty factors at kth iteration during the P2P negotiation process, respectively. The calculation and update process of dual variables and penalty factors associated with the P2P trading problem will be elaborated in (18) and (21), respectively.

Based on the C-ADMM algorithm, we can reformulate individual prosumer's optimization problem as follows:

$$\begin{aligned} \mathcal{L}_{t,i}^{\text{pro,k+1}}(x_{t,i}^{\text{pro}}, M_{t,ij}^k, \lambda_{t,ij}^{M,k}, \rho_{t,ij}^{M,k}) = &C_{t,i}^{\text{pro}}(x_{t,i}^{\text{pro}}, M_{t,ij}^k) \\ &+ \sum_M \sum_{j \in \omega_i} \left[\begin{array}{l} \lambda_{t,ij}^{M,k} (\frac{M_{t,ij}^k - M_{t,ji}^k}{2} - M_{t,ij}) \\ + \frac{\rho_{t,ij}^{M,k}}{2} (\frac{M_{t,ij}^k - M_{t,ji}^k}{2} - M_{t,ij})^2 \end{array} \right] \end{aligned} \tag{17a}$$

$$\left\{ x_{t,i}^{\text{pro,k+1}}, M_{t,i}^{\text{pro,k+1}} \right\} = \arg \min_{\left\{ x_{t,i}^{\text{pro}}, M_{t,i} \right\}} \mathcal{L}_{t,i}^{\text{pro}}(x_{t,i}^{\text{pro}}, M_{t,ij}^k) \tag{17b}$$

where $\mathcal{L}_{t,i}^{\text{pro,k+1}}(\cdot)$ is the augmented objective function of the prosumer connected to node i at $k+1th$ iteration. Each prosumer can update primal variables $\left\{ x_{t,i}^{\text{pro,k+1}}, M_{t,ij}^{k+1} \right\}$ according to (17).

The prosumers' dual variable update process is formulated as follows:

$$\lambda_{t,ij}^{M,k+1} = \left[\lambda_{t,ij}^{M,k} - \frac{\rho_{t,ij}^{M,k}}{2}\left(M_{ij}^{k+1} + M_{ji}^{k+1}\right)\right]^{+} \tag{18}$$

where the operator $[\cdot]^{+}$ is defined as $[\cdot]^{+} = \max(\cdot, 0)$.

Prosumers only need to submit their node power injection to DNO for system operation security concerns. The DNO will allocate necessary active power adjustments to prosumers to ensure NSCs. The operation model of DNO is shown as follows:

$$\begin{aligned}\mathcal{L}_t^{\mathrm{DNO},k+1}(P_{t,j}^{\mathrm{in},k}, Q_{t,j}^{\mathrm{in},k}) = &\left\| P_{t,j}^{\mathrm{in},k} + \Delta P_{t,j}^{\mathrm{in},k+1} + \sum_{i\in\Omega_j^{\mathrm{sup}}} P_{t,ij}^{\mathrm{line},k+1} - \sum_{m\in\Omega_j^{\mathrm{sub}}} P_{t,jm}^{\mathrm{line},k+1}\right\|_2^2 \\ &+ \left\| Q_{t,j}^{\mathrm{in},k} + \sum_{i\in\Omega_j^{\mathrm{sup}}} Q_{t,ij}^{\mathrm{line},k+1} - \sum_{m\in\Omega_j^{\mathrm{sub}}} Q_{t,jm}^{\mathrm{line},k+1}\right\|_2^2 + \gamma^{\mathrm{Adj}}(\Delta P_{t,j}^{\mathrm{in},k+1})^2\end{aligned} \tag{19a}$$

$$x_{t,i}^{\mathrm{DNO},k+1} = \arg\min_{x_{t,i}^{\mathrm{DNO}}} \mathcal{L}_t^{\mathrm{DNO},k+1}(P_{t,j}^{\mathrm{in},k}, Q_{t,j}^{\mathrm{in},k}) \tag{19b}$$

$$x_{t,i}^{\mathrm{DNO},k+1} := \left\{\mathbf{P}_t^{\mathrm{line},k+1}, \mathbf{Q}_t^{\mathrm{line},k+1}, \mathbf{V}^{k+1}, \Delta\mathbf{P}_t^{\mathrm{in},k+1}\right\} \tag{19c}$$

$$s.t. \begin{cases} V_{t,j}^{k+1} = V_{t,i}^{k+1} - (r_{ij}P_{t,ij}^{\mathrm{line},k+1} + x_{ij}Q_{t,ij}^{\mathrm{line},k+1}) \\ \underline{V} \le V_{t,j}^{k+1} \le \overline{V} \\ P_{t,i}^{\mathrm{in},k} + \Delta P_{t,i}^{\mathrm{in},k+1} = P_{t,i}^{\mathrm{Grid},k} + \sum\limits_g P_{t,i,g}^{\mathrm{DG},k} + \sum\limits_r P_{t,i,r}^{\mathrm{RES},k} - \sum\limits_m P_{t,i,m}^{\mathrm{L}} \\ P_{t,i}^{\mathrm{in},k} + \Delta P_{t,i}^{\mathrm{in},k+1} = E_{t,i}^{k} = \sum\limits_{j\in\omega_i} E_{t,ij}^{k} \\ Q_{t,i}^{\mathrm{in},k} = Q_{t,i}^{\mathrm{Grid},k} + \sum\limits_g Q_{t,i,k}^{\mathrm{DG},k} - \sum\limits_m Q_{t,i,m}^{\mathrm{L}} \\ \underline{P}_{ij}^{\mathrm{line}} \le P_{t,ij}^{\mathrm{line},k+1} \le \overline{P}_{ij}^{\mathrm{line}}, \underline{Q}_{ij}^{\mathrm{line}} \le Q_{t,ij}^{\mathrm{line},k+1} \le \overline{Q}_{ij}^{\mathrm{line}} \\ \Delta\underline{P}_{t,i}^{\mathrm{in}} \le \Delta P_{t,i}^{\mathrm{in},k+1} \le \Delta\overline{P}_{t,i}^{\mathrm{in}} \end{cases} \tag{19d}$$

where $\mathcal{L}_t^{\mathrm{DNO},k+1}(\cdot)$ is the augmented objective function of DNO at $k+1th$ iteration. DNO can update network variables $x_{t,i}^{\mathrm{DNO},k+1} := \left\{\mathbf{P}_t^{\mathrm{line},k+1}, \mathbf{Q}_t^{\mathrm{line},k+1}, \mathbf{V}^{k+1}, \Delta\mathbf{P}_t^{\mathrm{in},k+1}\right\}$ according to (19). $\Omega_j^{\mathrm{sup}}/\Omega_j^{\mathrm{sub}}$ are sets of upstream/downstream branches of node j, respectively. Note that variables with a superscript of k are the node injection power information provided by prosumers, i.e., they are given parameters to DNO. The calculation process of node injection power for individual prosumers is implemented by themselves to preserve their information privacy. Other variables with a superscript of $k+1$ are the network variables of DNO at $k+1th$ iteration.

The primal/dual local residuals and system residual are defined as follows:

$$pe_{t,i,M}^{k+1} = \sum_{j\in\omega_i}\left(M_{t,ij}^{k+1} + M_{t,ji}^{k+1}\right)^2, PE_{t,M}^{k+1} = \sum_{i\in\mathcal{N}^{\mathcal{B}}} pe_{t,i,M}^{k+1} \tag{20a}$$

$$de_{t,i,M}^{k+1} = \sum_{j\in\omega_i}\left(M_{t,ij}^{k+1} - M_{t,ij}^{k}\right)^2, DE_{t,M}^{k+1} = \sum_{i\in\mathcal{N}^{\mathcal{B}}} de_{t,i,M}^{k+1} \tag{20b}$$

$$\begin{aligned}NE_t^{k+1} = &\sum_{j\in\mathcal{N}^{\mathcal{B}}}\left\| P_{t,j}^{\mathrm{in},k} + \Delta P_{t,j}^{\mathrm{in},k} + \sum_{i\in\Omega_j^{\mathrm{sup}}} P_{t,ij}^{\mathrm{line},k} - \sum_{m\in\Omega_j^{\mathrm{sub}}} P_{t,jm}^{\mathrm{line},k}\right\|_2^2 \\ &+ \sum_{j\in\mathcal{N}^{\mathcal{B}}}\left\| Q_{t,j}^{\mathrm{in},k} + \sum_{i\in\Omega_j^{\mathrm{sup}}} Q_{t,ij}^{\mathrm{line},k} - \sum_{m\in\Omega_j^{\mathrm{sub}}} Q_{t,jm}^{\mathrm{line},k}\right\|_2^2\end{aligned} \tag{20c}$$

where $pe_{t,i,M}^{k+1}/de_{t,i,M}^{k+1}$ are the primal/dual local residuals of the prosumer connected to node i, $PE_{t,M}^{k+1}/DE_{t,M}^{k+1}$ are the summation of all prosumers' primal/dual local residuals during and NE_t^{k+1} is the system residual during $k+1th$ iteration at time slot t, respectively.

Self-adaptive penalty factor [35] is adopted to improve the convergence speed of the C-ADMM as (21) shows, where $\tau_{t,ij}^{M}$ is the correction parameter and $\omega_{t,ij}^{M}$ is the updating step parameter for the penalty factor $\rho_{t,ij}^{M,k}$ at time slot t, respectively. Different from existing researches like [20] and [22], we further decompose penalty factors into individual consensus constraint-level for enhancing privacy preservation, i.e., each consensus constraint will have an individual self-adaptive penalty factor. Therefore, the penalty factor updating process is implemented in a fully distributed fashion in this work as shown in (21).

$$\rho_{t,ij}^{M,k+1} = \begin{cases} \tau_{t,ij}^{M}\rho_{t,ij}^{M,k}, \left|pe_{t,M}^{k+1}\right| \ge \omega_{t,ij}^{M}\left|de_{t,M}^{k+1}\right| \\ \rho_{t,ij}^{M,k}/\tau_{t,ij}^{M}, \left|de_{t,M}^{k+1}\right| \ge \omega_{t,ij}^{M}\left|pe_{t,M}^{k+1}\right| \\ \rho_{t,ij}^{M,k}, \text{otherwise} \end{cases} \tag{21}$$

Remark 1: The choice of penalty factor $\rho_{t,ij}^{M,k}$ has a significant impact on the convergence performance of the ADMM-based distributed algorithm. Note that $\tau_{t,ij}^{M}/\omega_{t,ij}^{M}$ are given parameters of the prosumers according to their preference at each time slot t. The calculation of the penalty factor $\rho_{t,ij}^{M,k}$ can be explained as follows: 1) If the first condition of (21) is satisfied, then it means that the primal local residual exceeds the given tolerance, i.e., $\omega_{t,ij}^{M}\left|de_{t,M}^{k+1}\right|$. This situation implies that the primal local residual is far larger than the dual local residual. Therefore, at the next iteration decision process, the weighting factor $\rho_{t,ij}^{M,k}$ of the dual residual term $(\frac{M_{t,ij}^{k} - M_{t,ji}^{k}}{2} - M_{t,ij})^2$ in (17a) should be enlarged by $\tau_{t,ij}^{M}$ times to reduce the corresponding dual local residual. 2) If the second condition of (21) is satisfied, then it means that the dual local residual exceeds the given tolerance, i.e., $\omega_{t,ij}^{M}\left|pe_{t,M}^{k+1}\right|$. This situation implies that the dual local residual is far larger than the primal local residual. Therefore, at the next iteration decision process, the penalty factor $\rho_{t,ij}^{M,k}$ should be divided by $\tau_{t,ij}^{M}$. 3) If neither of the above two conditions is satisfied, the penalty factor $\rho_{t,ij}^{M,k}$ will remain unchanged.

According to [35], as long as the objective function is convex, the convergence of the ADMM method is ensured to finally converge to the global optimal point. Thus, the joint E&R&C P2P trading market converges as long as the summation of all prosumers' primal and dual residuals fall below stopping criteria according to [35] for each kind of trading merchandise and the system residual falls below stopping criteria as well. The stopping condition is given as (22).

$$\begin{cases} PE_{t,M}^{k+1} \leqslant \delta_M^{\mathrm{PE}}, DE_{t,M}^{k+1} \leqslant \delta_M^{\mathrm{DE}} \\ NE_t^{k+1} \leqslant \delta^{\mathrm{DN}} \end{cases} \tag{22a}$$

$$PE_{t,M}^{k} = \left\{PE_{t,\mathrm{E}}^{k}, PE_{t,\mathrm{R,U}}^{k}, PE_{t,\mathrm{R,D}}^{k}, PE_{t,\mathrm{CER}}^{k}\right\} \tag{22b}$$

$$DE_{t,M}^{k} = \left\{DE_{t,\mathrm{E}}^{k}, DE_{t,\mathrm{R,U}}^{k}, DE_{t,\mathrm{R,D}}^{k}, DE_{t,\mathrm{CER}}^{k}\right\} \tag{22c}$$

$$\delta_M^{\mathrm{PE}} = \left\{\delta_{\mathrm{E}}^{\mathrm{PE}}, \delta_{\mathrm{R,U}}^{\mathrm{PE}}, \delta_{\mathrm{R,D}}^{\mathrm{PE}}, \delta_{\mathrm{CER}}^{\mathrm{PE}}\right\} \tag{22d}$$

$$\delta_M^{\mathrm{DE}} = \left\{\delta_{\mathrm{E}}^{\mathrm{DE}}, \delta_{\mathrm{R,U}}^{\mathrm{DE}}, \delta_{\mathrm{R,D}}^{\mathrm{DE}}, \delta_{\mathrm{CER}}^{\mathrm{DE}}\right\} \tag{22e}$$

We further develop an accelerated C-ADMM algorithm based on the GSA method [36] to enhance algorithm smoothness and efficiency. Based on the information from previous iterations, we can define a correction coefficient by calculating

the adjacent gradient as follows:

$$g_{t,i}^{M,k+1}=\frac{\left\|Z_{t,i}^{k+1}-M_{t,i}^{k}\right\|_2}{\left\|M_{t,i}^{k}-M_{t,i}^{k-1}\right\|_2} \tag{23a}$$

$$\begin{cases}\beta_t^{M,k+1}=\frac{1+\sqrt{1+4(\beta_t^{M,k})^2}}{2}\\ \alpha_t^{M,k+1}=\frac{\beta_t^{M,k}-1}{\beta_t^{M,k+1}}\\ \varphi_{t,i}^{M,k+1}=\alpha_t^{M,k+1}\frac{g_{t,i}^{M,k+1}}{1-g_{t,i}^{M,k+1}}\end{cases} \tag{23b}$$

where $Z_{t,ij}^{k+1}$ is the $M_{t,ij}^{k+1}$ derived in (17), which hasn't been accelerated. We use $Z_{t,ij}^{k+1}$ as an auxiliary variable to update the primal variable in our proposed accelerated algorithm. $\beta_t^{M,k+1},\alpha_t^{M,k+1}$ are the Nesterov acceleration variables inspired by Nesterov's acceleration method [28] and $g_{t,i}^{M,k+1},\varphi_{t,i}^{M,k+1}$ are the GSA acceleration variables.

Remark 2: The main idea of the GSA method is to utilize the gradient information as shown in (23a) calculated by the geometric series to update the variables. We further modify the correction factor of the gradient acceleration term by using adaptive variable $\alpha_t^{M,k}$ rather than fixed constant in [36] for better computation efficiency.

Therefore, we reformulate (17b) as (24):

$$\begin{aligned}\left\{x_{t,i}^{\text{pro,k+1}},Z_{t,ij}^{k+1}\right\}=&\arg\min_{\left\{x_{t,i}^{\text{pro}},M_{t,ij}\right\}}C_{t,i}^{\text{pro}}(x_{t,i}^{\text{pro}})\\&+\sum_M\sum_{j\in\omega_i}\begin{bmatrix}\lambda_{t,ij}^{M,k}(\frac{M_{t,ij}^k-M_{t,ji}^k}{2}-M_{t,ij}^k)\\+\frac{\rho^{M,k}}{2}(\frac{M_{t,ij}^k-M_{t,ji}^k}{2}-M_{t,ij}^k)^2\end{bmatrix}\end{aligned} \tag{24a}$$

$$M_{t,ij}^{k+1}=Z_{t,ij}^{k+1}+\underbrace{\varphi_t^{M,k+1}(Z_{t,ij}^{k+1}-M_{t,ij}^k)}_{\text{geometric series term}}+\underbrace{\gamma_t^M(M_{t,ij}^k-M_{t,ij}^{k-1})}_{\text{heavy ball term}} \tag{24b}$$

where γ_t^M is the coefficient for the introduced heavy ball acceleration [27] term for enhancing the smoothness of the proposed algorithm.

The implementation algorithm for the proposed P2P trading mechanism is shown in Algorithm 1. The preliminary step is system parameters initialization. Then, at time slot t, the first step is to determine each prosumer's reserve requirements and initialize P2P E&R&C trading strategies $M_{t,ij}^0$, corresponding dual variables $\lambda_{t,ij}^{M,0}$ and penalty factors $\rho_{t,ij}^{M,0}$. Next, the iterative process of the prosumers and DNO begins. Each prosumer needs to update their P2P trading strategies and exchange the updated P2P trading information with their trading partners. Corresponding dual variables will be updated accordingly. After all the prosumers finish their update process, prosumers only need to submit their node injection power to DNO for system security concerns. DNO will verify the feasibility of the P2P transactions between prosumers in physical DN and allocate necessary node power adjustments to certain prosumers to ensure system operation security. And then the system residual and P2P trading primal and dual residuals are calculated to check whether the P2P trading market has converged or not. Self-adaptive penalty factors will be updated if the algorithm hasn't converged.

Algorithm 1 Implementation Algorithm for the Proposed P2P Trading Mechanism

Initialize parameters.
for $t=1$ to T **do**
  Prosumer connected to node i**:**
  ◇ *Prosumer-level Reserve Determination*:
  Determines $R_{t,i,r}^{\text{RES,D}},R_{t,i,r}^{\text{RES,U}}$ by (5) and $R_{t,i,m}^{\text{Load,D}},R_{t,i,m}^{\text{Load,U}}$ by (31).
  Initialize $\left\{M_{t,ij}^0,\lambda_{t,ij}^{M,0},\rho_{t,ij}^{M,0}\right\}$ and set $k=0$.
  while $k<k_{max}$ **do**
    Prosumer connected to node i**:**
    ◇ *Prosumer Decisions Update*:
    if $k>1$ **then**
      Updates $\left\{x_{t,i}^{\text{pro,k+1}},M_{t,ij}^{k+1}\right\}$ by (23)-(24).
    else
      Updates $\left\{x_{t,i}^{\text{pro,k+1}},M_{t,ij}^{k+1}\right\}$ by (17).
    end if
    ◇ *P2P Trading Negotiation Process*:
    Exchanges $\left\{M_{t,ij}^{k+1},M_{t,ji}^{k+1}\right\}$ with prosumer $j\in\omega_i$.
    Updates $\lambda_{t,ij}^{M,k+1}$ by (18).
    DNO:
    ◇ *Prosumer Node Injection Power Information*:
    Receives $\left\{P_{t,j}^{\text{in},k},Q_{t,j}^{\text{in},k}\right\},\forall j\in\mathcal{N}^{\mathcal{B}}$ from prosumers.
    ◇ *DNO Decisions Update*:
    Updates $x_{t,i}^{\text{DNO},k+1}$ by (19).
    ◇ *DNO Power Adjustments*:
    Allocates $\Delta P_{t,j}^{\text{in},k},\forall j\in\mathcal{N}^{\mathcal{B}}$ to prosumers.
    Convergence Analysis:
    Calculate residuals by (20).
    if Stopping condition (22) is satisfied **then**
      Break
    else
      Update penalty factors by (21).
    end if
    Update iteration index $k=k+1$.
  end while
end for

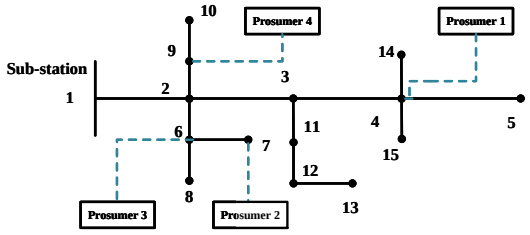

Fig. 2. Topology of the IEEE 15-Bus distribution system with 4 prosumers.

V. SIMULATION STUDIES

A. Simulation Setup

Numerical simulations are conducted to verify the effectiveness of the proposed P2P joint E&R&C trading market mechanism. All the simulations are conducted on a 64-bit Windows environment laptop with Intel(R) Core(TM) i5-12500H 3.10 GHz CPU and 16 GB RAM. The models are coded in MATLAB 2021b with the YALMIP toolbox and solved by the Gurobi 10.0 solver.

B. IEEE 15-Bus distribution system

We conduct numerical tests on the IEEE 15-Bus distribution system in this case study. The topology of the test system is

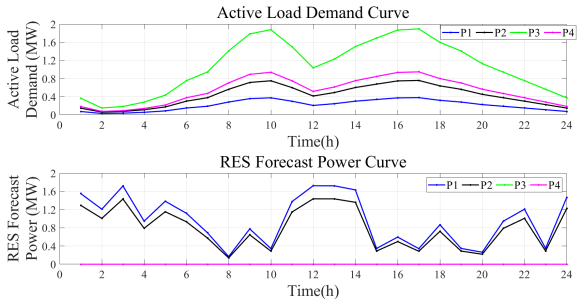

Fig. 3. Active load demand and maximum RES forecast power curves of the prosumers.

shown in Fig. 2. The active load demand curves and maximum RES forecast power curves are shown in Fig. 3. The load demand and RES power curves are modified based on the data of [37]. The total daily load energy demand and RES energy generation forecast values are 53.92 MWh and 42.32 MWh, respectively. We define the RES penetration level φ^{RES} as the total daily RES energy generation forecast value divided by the total load energy demand forecast value in this work. Thus, φ^{RES} in Case I - Case V is 78.5%. The total carbon emission quantity of the system is defined as the summation of the carbon emission caused by the carbon-intensive DG power generation and the purchasing power from the upstream grid.

The system base capacity is 1 MVA and the base voltage is 11 kV. The active/reactive load demand of normal nodes which doesn't have prosumers are also taken into consideration without loss of generality. 4 prosumers (denoted as P1, P2, P3, P4, respectively) are connected to nodes 4,7,6,9 of the system, respectively. We set all the convergence criteria parameters $\left\{\delta_M^{\mathrm{PE}}, \delta_M^{\mathrm{DE}}, \delta^{\mathrm{DN}}\right\}$ as 10^{-5} in this case study. The P2P energy/reserve trading price is set to be half of the upstream energy/reserve price. The feed-in tariff is set to be zero. The typical chosen values of $\omega_{t,ij}^M/\tau_{t,ij}^M$ can be selected as 10/2 according to [35], respectively. Other detailed parameters are provided in datasheet [38] due to page limit.

1) Ambiguity Set Formulation: The Monte Carlo simulation approach is used to generate 50000 scenarios of RES power forecast error following the multivariate Gaussian distribution $\mathcal{N}(\mu, \mathbf{\Sigma})$. The parameter settings of $\mathcal{N}(\mu, \mathbf{\Sigma})$ are shown as follows:

$$\begin{cases} \mathbf{\Sigma}_{i,i} = \zeta \sum\limits_{r} P_{t,i,r}^{\mathrm{RES}} \\ \mathbf{\Sigma}_{i,j} = \rho_{ij} \zeta \sum\limits_{r} P_{t,i,r}^{\mathrm{RES}} \sum\limits_{r} P_{t,j,r}^{\mathrm{RES}} \end{cases} \tag{25}$$

Note that we set $\mu = \mathbf{0}$, $\zeta = 0.02$ and $\rho_{ij} = 0.05$ in all the simulations for the RES uncertainty ambiguity formulation. We randomly select 500 samples out of the generated 50000 scenarios to form the training data (in-sample data) as the historical information of RES power forecast errors. The rest of them form the test data (out-of-sample data) to verify the effectiveness of the strategies under the stochastic environment in the real world. The load uncertainty ambiguity formulation is similar to the RES uncertainty ambiguity formulation process. The detailed process is shown in Appendix-A.

2) Convergence Performance Comparisons with Different Distributed Algorithms: We compare the convergence performance of the proposed accelerated C-ADMM algorithm based on geometric series acceleration (GSA) method (denoted as GSAC-ADMM) with different distributed algorithms like C-ADMM [20], [22], [35] and C-ADMM based on heavy ball acceleration method [27] (denoted as HBAC-ADMM), C-ADMM based on Nesterov acceleration method [28] (denoted as NAC-ADMM). Note that all the distributed algorithms used in comparisons adopt the same fully distributed penalty factor update process as shown in (21) of the proposed GSAC-ADMM algorithm for the consistency concern.

TABLE II
DIFFERENT ALGORITHMS' CONVERGENCE PERFORMANCE COMPARISONS IN THE IEEE 15-BUS DISTRIBUTION SYSTEM

Item	C-ADMM	HBAC-ADMM	NAC-ADMM	GSAC-ADMM
Convergence Iterations	20	20	20	17
Computational Time (s)	32.43	29.95	29.84	25.51
Maximum P2P Trading Optimality Gap	0.60%	0.56%	0.51%	0.38%
Maximum Prosumer Cost Optimality Gap	0.83%	0.73%	0.66%	0.37%

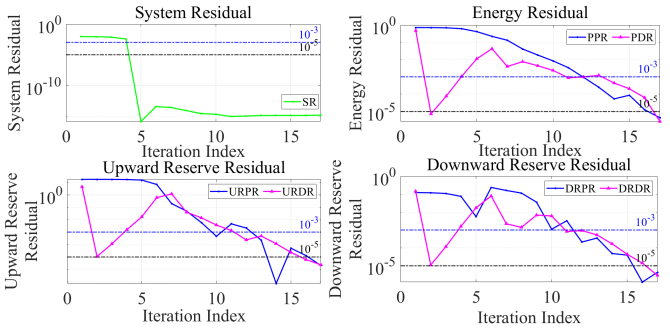

Fig. 4. Primal and Dual residuals iteration process of the proposed GSAC-ADMM algorithm.

To evaluate the algorithm accuracy criteria, the P2P trading and prosumer cost optimality gaps of the distributed solution are defined as follows:

$$\varepsilon_{t,ij}^{M,\mathrm{Gap}} = \frac{\left|M_{t,ij}^{*,\mathrm{Dis}} - M_{t,ij}^{*,\mathrm{Cen}}\right|}{\left|M_{t,ij}^{*,\mathrm{Cen}}\right|} \times 100\% \tag{26a}$$

$$\varepsilon_{t,i}^{\mathrm{obj,Gap}} = \frac{\left|C_{t,i}^{\mathrm{pro}}(x_{t,i}^{*,\mathrm{pro,Dis}}) - C_{t,i}^{\mathrm{pro}}(x_{t,i}^{*,\mathrm{pro,Cen}})\right|}{\left|C_{t,i}^{\mathrm{pro}}(x_{t,i}^{*,\mathrm{pro,Cen}})\right|} \times 100\% \tag{26b}$$

where $\varepsilon_{t,ij}^{M,\mathrm{Gap}}$ is the P2P trading optimality gap of the distributed solution $M_{t,ij}^{*,\mathrm{Dis}}$ compared with the centralized optimal solution $M_{t,ij}^{*,\mathrm{Cen}}$. $\varepsilon_{t,i}^{\mathrm{obj,Gap}}$ is the prosumer cost optimality gap of the distributed solution $x_{t,i}^{*,\mathrm{pro,Dis}}$ compared with the centralized optimal solution $x_{t,i}^{*,\mathrm{pro,Cen}}$.

Table II shows that the proposed GSAC-ADMM algorithm outperformed other comparison algorithms both in computation efficiency and accuracy aspects. Thus, the numerical tests have verified the advantages of the proposed algorithm in implementing efficient P2P trading between prosumers.

Remark 3: About the algorithm computational time aspect, since we only use one solver to implement the decision-making of each prosumer and DNO, the algorithm is implemented in a sequential computing manner in this work. In practical application, each prosumer and DNO can use their individual computation unit to complete individual decision making and the algorithm can be implemented in a parallel computing manner, which can further reduce the computational time.

Fig. 4 shows the primal and dual residuals iteration process

TABLE III
COMPARISONS OF POWER UTILIZATION IN THE IEEE 15-BUS DISTRIBUTION SYSTEM

Item	Case I	Case II	Case III
Main Grid Power (MW)	17.66	19.82	15.06
P2P Trading Power (MW)	41.71	37.39	46.90
DG Generation Power (MW)	10.30	9.88	11.79
RES consumption Power (MW)	25.96	24.22	27.07

TABLE IV
COMPARISON OF THE PROSUMERS' OPERATION COSTS IN THE IEEE 15-BUS DISTRIBUTION SYSTEM

Prosumer Index	P1	P2	P3	P4
Operation Cost ($) in Case I	3823.24	3647.32	7672.54	4168.45
Operation Cost ($) in Case II	3854.23	2937.87	4234.23	2462.11

of the proposed GSAC-ADMM algorithm at 16:00, including system residual (SR), energy primal/dual residual (EPR/EDR), upward reserve primal/dual residual (URPR/URDR) and downward reserve primal/dual residual (DRPR/DRDR). We can see that the proposed method can achieve good convergence performance, the primal and dual residuals fall below 10^{-3} around $15th$ iteration.

3) P2P Trading Mechanism Comparison Case Studies: We conduct comparison case studies with other P2P trading mechanisms to verify the advantages and effectiveness of the established P2P joint E&R&C trading market considering NSCs and uncertainty. The setup for cases are listed as follows:

- *Case I:* The proposed P2P joint E&R&C trading mechanism as described in previous sections.
- *Case II:* P2P joint E&R trading mechanism as in [20], [22]. In this case, the carbon emission impact of the prosumers' P2P transactions is not considered.
- *Case III:* Financial-oriented P2P trading mechanism. In this case, prosumers only focus on financial benefits during P2P transactions. The NSCs of DN are neglected.
- *Case IV:* P2P trading mechanism using single-sided DRCC (SS-DRCC) method as in [39] to solve the reserve determination problem.
- *Case V:* P2P trading mechanism using SO method as in [19] to solve reserve determination problem.

The comparisons of system power utilization under Cases I-III are shown in Table III. It can be seen that Case III (Financial-oriented) achieves the highest RES power consumption while Case I (Proposed) achieves higher RES power consumption than Case II (Without carbon emission impact concern). The reason behind the results is that Case III only focuses on the economic aspects of P2P trading and doesn't consider the NSCs of the DN system. We further verify the system branch active power flow profile and node voltage profile by applying the P2P transaction strategies derived in Case III and compare the results with that of Case I as shown in Fig. 5. The figure shows that if we choose to apply the P2P trading strategies derived in Case III, though the system node voltage maintains within safe operation range, the branch active power flow will exceed the branch active power flow capacity significantly. The maximum branch active power flow in Case III is 1.02 MW (70% higher than line capacity upper bound). Therefore, we can get the conclusion that considering the NSCs of the DN system during P2P transactions is of great importance to ensure the security of system operation. The proposed P2P trading mechanism considers NSCs can achieve good performance in both economic and technical (system security) aspects.

From the comparison between Case I and Case II, we can see that Case I increases RES power consumption by 4.32% and decreases grid purchasing power by 10.90% compared with Case II. Moreover, the system total P2P energy trading power in Case I is 11.56% higher than that of Case II. Thus it can be concluded that taking the carbon emission impact of P2P energy transactions can improve system low carbon emission power utilization by consuming more RES power instead of relying on the exogenous power supply. Besides the power utilization aspect, we further investigate the impact of P2P CER trading, prosumers' operation costs in Case I and Case II are shown in Table IV. We can find that prosumers with higher RES power consumption will be rewarded with extra CERs to get more benefits in the P2P CER trading market (e.g. P1 with cost reduction by 0.81%). On the contrary, prosumers with higher carbon-intensive DG power generation will face higher operation costs by purchasing CERs and receiving CER penalty costs (e.g. P2 with cost increasement by 24.15%). Moreover, the carbon emission obligation of demand-side users (e.g. P3 and P4) is also implemented in the proposed P2P CER trading market. Therefore, we can get the conclusion that the P2P CER trading market can further improve the fairness of the carbon emission obligation problem between the electricity generation side and the demand side.

We compare Case I, Case IV and Case V from the aspect of the uncertainty-resilience performance. Note that both the uncertainties of RES and load are considered in the case studies. SO method in Case V is chosen as the benchmark case in this part. The simulation results show that the daily reserve power derived by the SO method is 12.97 MW with the in-sample and out-of-sample constraint violation probability of 66.40% and 64.47%, respectively. The out-of-sample performance in Case V is better than that of in-sample performance because out-of-sample data covers more types of the uncertainty scenarios. The same conclusion can be derived in Case I and Case IV as shown in Fig. 6. It can be found that the performance of the SO method is very poor due to limited training samples. The only way to improve the performance of the SO method is to add more training samples. However, it will inevitably lead to high computation complexity if the training data set is enlarged. Different from the SO method relying on exact scenario realization, the DRCC method can exploit the inherent information about uncertainty described in ambiguity set to guide the decision process. As Fig. 6 shows, the DRCC method can achieve reliable but not over-conservative strategies against uncertainty with limited information. We can see that the strategy derived by Case I using the TS-DRCC method can achieve better robustness performance than that of Case IV using the SS-DRCC method under different risk preference parameters. Moreover, as the risk preference parameter increases, the constraint violation probability difference between the two methods will be more significant, which can further demonstrate the advantages of the adopted TS-DRCC method.

4) Simulation Results and Analysis: The daily P2P joint energy, upward/downward reserve and CER trading profiles

among prosumers in Case I are shown in Fig. 7. The following conclusions for different types of P2P trading merchandises can be derived:

i)P2P Energy trading: Prosumers with load demand prefer purchasing active power from other prosumers with excessive RES power generation. P2P energy trading quantity accounts for 77.35% of total active load demand and the ratio of RES consumption power in total power utilization is 48.14% higher than that of DG generation power. This is because the P2P energy trading price is lower than the grid energy purchasing price and the generation costs of DGs are higher than that of RESs. This kind of pricing mechanism can improve local RES consumption and promote energy sharing between prosumers. Besides this, the network usage charge will motivate prosumers to implement P2P energy transactions with less power transmission loss, which can further improve the operation performance of the DN.

ii)P2P Reserve Trading: P2P reserve trading quantity accounts for 64.34% of total reserve capacity requirements. Thus, the proposed prosumer-level reserve determination and scheduling method can significantly reduce the reserve capacity burden of DNO. Moreover, the joint constraints of DG generation power and upward/downward reserve capacity can limit prosumers' reserve capacity bidding quantities in the reserve market. This can ensure the reliability of the prosumers providing upward/downward reserve capacity during the P2P trading process.

iii)P2P CER Trading: Prosumers will be rewarded with extra CERs to get more profits by participating in the P2P CER trading market for utilizing RES power. Load consumption and high-pollution DG generation will be charged with a certain amount of CERs since both consumption and generation sides are allocated with carbon emission responsibility. Particularly, prosumers will need to pay CER penalty costs if they can't compensate for their CER requirements in the P2P CER trading market. The CER penalty price is set to be higher than the P2P CER trading price to encourage low-carbon power consumption. 41.41% of the total P2P CER trading is completed during 11:00-14:00 when RES power consumption is significant. Thus, it demonstrates that establishing a P2P CER trading market can further promote RES power utilization.

iv)Analysis on the impact of the P2P CER Trading under different φ^{RES}: We conducted numerical simulations with different φ^{RES} ranging from 0.2-0.8 with the changing step size of 0.2. We compared the total carbon emission quantity and P2P trading power of the system under these scenarios. The results are shown in Table V. To further investigate the impact of P2P CER trading with different φ^{RES}, we have also calculated the total carbon emission reduction rate and P2P trading power increasement rate as shown in Table V.

From the results, we can find that under each given φ^{RES} scenario, the proposed P2P CER trading can both reduce the total carbon emission and promote P2P trading among prosumers. Two interesting findings can be found from two aspects including the carbon emission reduction rate and the P2P trading power increasement rate:

1) As the φ^{RES} continues to grow, we can also find that the carbon emission reduction rate also increases. This is because as the φ^{RES} increases, more carbon-intensive power supply such as DG power generation and upstream purchasing power can be replaced by clean RES power under the proposed P2P CER trading mechanism.

2) As for the P2P trading power increasement aspect, we can find that the P2P trading power increasement rate grows as the φ^{RES} grows ranging from 20% to 60%.

However, the P2P trading power increasement rate decreases when the φ^{RES} grows from 60% to 80%. Moreover, it can also be found that the carbon emission reduction increasement with the φ^{RES} changing from 60% to 80% is lower than other scenarios changing from 20% to 60%. The reason is that when the φ^{RES} is relatively low, e.g., 20%, the RES power consumption potential of P2P energy sharing considering the CER trading is relatively high. As the φ^{RES} continues to grow, the carbon reduction and P2P trading promotion potential of the system will decrease as well. Finally, when the φ^{RES} is nearly saturated compared with the load demand, e.g., 80%, then the RES consumption of the system is also nearly saturated. The physical constraints like power flow constraints during the power system operation will restrict the power-sharing between prosumers located at different nodes, e.g., we can find that the branch power flow nearly reaches the line capacity lower bound as shown in Fig. 5. Thus the RES consumption will approach the saturated value if the physical network operation constraints are binding.

Therefore, the positive impact of the P2P CER trading mechanism to the low-carbon transition of the power system is still quite promising since the φ^{RES} is still increasing and the RES consumption rate of the system hasn't reached the saturated value yet.

v)Analysis of the impact of the uncertain upstream electricity price: The uncertainty modeling of the upstream electricity price and RO-based prosumer optimization model is elaborated in Appendix-B for the paper's clarity. The maximum deviation of the upstream electricity price is set to be 5%. The results are shown in Table VI.

It can be observed that by considering the uncertainty of the upstream electricity price using the RO method as in [40], the components of the power utilization of the system and the prosumer's operation costs will be changed. Since the RO method considers the worst scenario of uncertainty, the prosumers decrease the purchasing power from the upstream grid by 1.94%. Due to the MMR pricing scheme, the prosumers tend to satisfy their load demand through P2P trading for lower operation costs. Therefore, the total P2P trading power and DG generation power increase by 1.64% and 3.33%, respectively. The total RES consumption power under two scenarios is the same because the cost for RES power utilization is the lowest and prosumers will be charged with RES curtailment costs. Therefore, prosumers tend to replace upstream purchasing power of higher price with P2P trading power of lower price instead. It can be observed that the operation costs of prosumers (P1, P2, and P3) increase 1.66%, 1.53%, and 3.24% under the RO scenario compared with the deterministic scenario. respectively. This is caused by considering the worst scenario of the upstream electricity price. The operation cost of prosumer P2 hasn't changed too

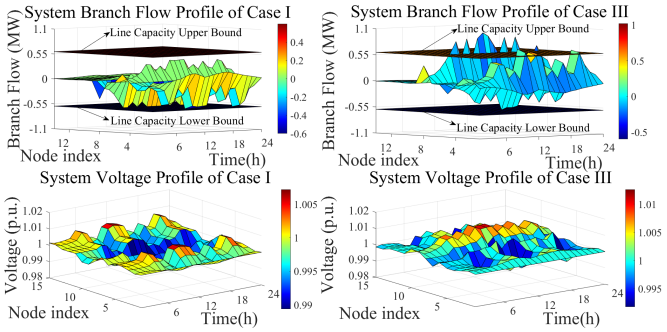

Fig. 5. System branch power flow and node voltage profile of Case I and Case III.

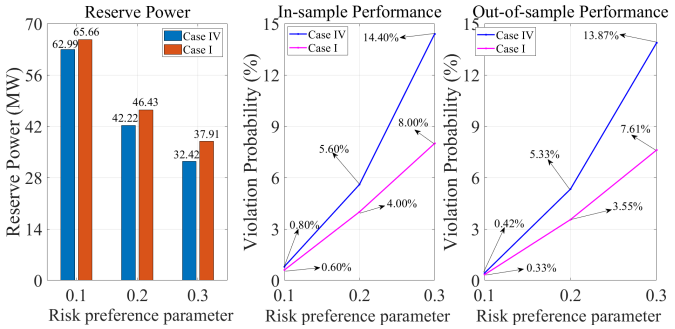

Fig. 6. Reserve power and uncertainty-resilience performance comparison of Case I and Case IV.

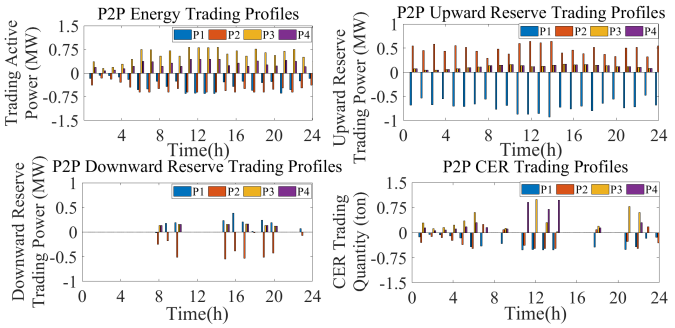

Fig. 7. P2P trading profiles.

TABLE V
COMPARISON OF CARBON EMISSION REDUCTION RATE AND P2P TRADING POWER INCREASEMENT RATE WITH DIFFERENT φ^{RES}

φ^{RES}	20%	40%	60%	80%
Total Carbon Emission Quantity in Case I (ton)	48.16	40.33	34.69	33.26
Total Carbon Emission Quantity in Case II (ton)	48.52	41.61	36.91	33.46
Total P2P Trading Power in Case I (MW)	33.37	37.31	40.14	41.85
Total P2P Trading Power in Case II (MW)	29.99	32.80	34.97	37.58
Carbon Emission Reduction Rate[1]	0.73%	3.09%	6.00%	6.55%
P2P Trading Power Increasement Rate[2]	11.27%	13.75%	14.78%	11.38%

Carbon Emission Reduction Rate[1]: The total carbon emission quantity reduction rate of Case I compared with that of Case II.
P2P Trading Power Increasement Rate[1]: The total P2P Trading Power increasement rate of Case I compared with that of Case II.

much under these two scenarios because it mainly consumes RES power.

TABLE VI
COMPARISONS OF POWER UTILIZATION IN THE IEEE 15-BUS DISTRIBUTION SYSTEM UNDER DETERMINISTIC AND RO SCENARIOS

Item	Deterministic Scenario[1]	RO Scenario[2]
Main Grid Power (MW)	17.66	17.32
P2P Trading Power (MW)	41.71	42.39
DG Generation Power (MW)	10.30	10.65
RES consumption Power (MW)	25.96	25.96
P1 Operation Cost ($)	3823.24	3822.82
P2 Operation Cost ($)	3647.32	3707.89
P3 Operation Cost ($)	7672.54	7789.58
P4 Operation Cost ($)	4168.45	4303.52

Deterministic Scenario[1]: The uncertainties of the load and RES are considered by using the TS-DRCC-based method and the upstream electricity price is deterministic.).
RO Scenario[2]: The uncertainties of the load and RES are considered by the TS-DRCC-based method and the upstream electricity price is considered by using RO based method.

TABLE VII
DIFFERENT ALGORITHMS' CONVERGENCE PERFORMANCE COMPARISONS ON THE IEEE 141-BUS DISTRIBUTION SYSTEM

Item	C-ADMM	HBAC-ADMM	NAC-ADMM	GSAC-ADMM
Convergence Iterations	35	32	33	32
Computational Time (s)	181.06	164.50	158.33	150.47
Maximum P2P Trading Optimality Gap	5.79%	5.71%	5.08%	1.84%
Maximum Prosumer Cost Optimality Gap	0.33%	0.29%	0.15%	0.03%

C. IEEE 141-Bus distribution system

We conduct numerical simulations on the IEEE 141-Bus distribution system with 8 prosumers to further demonstrate the scalability and advantages of the proposed algorithm. The base capacity of the IEEE 141-Bus distribution system is 10 MVA and the base voltage is 12.47 kV. Note that in this case, we set all the convergence criteria parameters as 10^{-6}. Table VII shows the comparison results of the proposed algorithm and other comparison algorithms. The test results have verified the advantages of the proposed algorithm both in computation efficiency and accuracy aspects. It can be seen that the proposed GSAC-ADMM algorithm can achieve higher computation efficiency and accuracy compared with other algorithms in large-scale system applications. Therefore, the proposed algorithm can promote P2P joint E&R&C trading market development for the future power system with high penetration DERs.

VI. CONCLUSION

This paper proposes a carbon-aware P2P joint energy and reserve trading market considering NSCs for prosumers. To handle the uncertainties associated with loads and RESs. A prosumer-level reserve determination method is proposed to enhance the fairness of reserve responsibility obligation among the DNO and prosumers. In addition, to improve the operation efficiency of the proposed P2P joint E&R&C trading market, an accelerated C-ADMM algorithm based on the GSA method with the fully distributed self-adaptive penalty factor is proposed. Finally, the proposed method is tested on both small-scale and large-scale IEEE distribution systems. The major conclusions and findings are listed as follows:

- The test results demonstrate that the proposed TS-DRCC-based prosumer-level reserve determination method can reduce the reserve constraint violation probability by at most 6.6% compared with the SS-DRCC-based approach

in [39]. Moreover, as each prosumer can evaluate its reserve requirement independently in the proposed method, the information and decision privacy of each prosumer can be further enhanced.

- The GSA method accelerated C-ADMM algorithm outperforms other comparison distributed algorithms in both computation efficiency and accuracy aspects. Furthermore, the proposed fully distributed self-adaptive penalty factor can better protect the parameter privacy for each pair of P2P trading partners during the market operation process.
- Low-carbon power generation and consumption can be further promoted by considering the carbon emission impact of P2P transactions. The proposed P2P CER trading market can increase the system total P2P trading power/total RES consumption power by 11.55%/7.18% and decrease the system total carbon emission quantity by 6.45%.

Some parts of this work can be further improved. Firstly, the communication failure among prosumers hasn't been considered during the P2P negotiation process. Further, the information privacy of the prosumers needs better protection. Given the aforementioned research drawbacks, future work can focus on enhancing the resilience of the distributed algorithm against communication failure. Moreover, developing an encryption mechanism to further enhance the security of individual prosumer's information privacy is also a promising way to promote the development of P2P trading.

APPENDIX

A. Considering the Uncertainty Associated with Load

Similar to the ambiguity set description of the uncertain RES power forecast error, the uncertain load power forecast error can be described by the ambiguity set $\mathcal{P}^d$ given as:

$$\mathcal{P}^d := \{\mathbb{P}_{\sigma_t} : \mathbb{E}_{\mathbb{P}}[\sigma_t] = \mu^d, \mathbb{E}_{\mathbb{P}}[(\sigma_t - \mu^d)(\sigma_t - \mu^d)^\top] = \Sigma^d\} \tag{27}$$

where $\mathbb{E}_{\mathbb{P}}$ denotes the expectation operator and σ_t is the load power forecast error at time slot t, $\mu^{\mathbf{d}}$ and $\mathbf{\Sigma^d}$ are mean value vector and covariance matrix of σ_t, respectively.

The upward/downward reserve requirements of the prosumer with load located at node i are defined as follows:

$$\sigma_t = \sigma_t^+ - \sigma_t^- \tag{28a}$$

$$e_i^d[m] = \begin{cases} 0, m \neq i \\ 1, m = i \end{cases} \tag{28b}$$

$$R_{t,i,m}^{\text{Load,U}} = {e_i^d}^\top \xi_t^-, R_{t,i,m}^{\text{Load,D}} = {e_i^d}^\top \sigma_t^+ \tag{28c}$$

where (28a) means that the load power deviation can be divided into two parts including upward/downward deviation denoting increase/decrease power of load, respectively. (28b) defines the load indicator vector of size ($\mathcal{N}^{\mathcal{B}} \times 1$) for prosumer located at node i, $\mathcal{N}^{\mathcal{B}}$ is the number of system nodes and $e_i^d[m]$ is the mth element of e_i^d. (28c) contains the upward/downward reserve requirements defined as $R_{t,i,m}^{\text{Load,U}}$ / $R_{t,i,m}^{\text{Load,D}}$ at time slot t.

Considering the uncertainty of loads, the load reserve determination problem for individual prosumer located at node i is formulated as follows:

$$\min \sum_m (R_{t,i,m}^{\text{Load,D}} + R_{t,i,m}^{\text{Load,U}}) \tag{29a}$$

$$s.t. \inf_{\mathbb{P}_{\sigma_t} \in \mathcal{P}^d} \mathbb{P}_{\sigma_t}[-R_{t,i,m}^{\text{RES,U}} \leqslant {e_i^d}^\top \sigma_t \leqslant R_{t,i,m}^{\text{RES,D}}] \geqslant 1 - \varepsilon_i \tag{29b}$$

where ε_i is the risk preference parameter of the prosumer located at node i describing the probability of not satisfying reserve requirement constraint.

The generic symmetrical TS-DRCC for (29b) can be given as follows:

$$\inf_{\mathbb{P}_{\sigma_t} \in \mathcal{P}} \mathbb{P}_{\sigma_t}[-T_1(x_{t,i,m}^{\text{Load,R}}) \leqslant {e_i^d}^\top \sigma_t - T_2(x_{t,i,m}^{\text{Load,R}}) \leqslant T_1(x_{t,i,m}^{\text{Load,R}})] \geqslant 1 - \varepsilon_i \tag{30a}$$

$$x_{t,i,m}^{\text{Load,R}} = \{R_{t,i,m}^{\text{Load,D}}, R_{t,i,m}^{\text{Load,U}}\} \tag{30b}$$

$$T_1(x_{t,i,m}^{\text{Load,R}}) = \frac{R_{t,i,m}^{\text{Load,D}} + R_{t,i,m}^{\text{Load,U}}}{2}, T_2(x_{t,i,m}^{\text{Load,R}}) = \frac{R_{t,i,m}^{\text{Load,D}} - R_{t,i,m}^{\text{Load,U}}}{2} \tag{30c}$$

The origin intractable problem can be reformulated as tractable second-order cone (SOC) form as follows:

$$\min \sum_m (R_{t,i,m}^{\text{Load,D}} + R_{t,i,m}^{\text{Load,U}}) \tag{31a}$$

$$s.t. \left\{ \begin{array}{c} q^2 + {e_i^d}^\top \mathbf{\Sigma^d} e_i^d \leq \varepsilon_i \Big(T_1(x_{t,i,m}^{\text{Load,R}}) - z\Big)^2 \\ -(q+z) \leq -T_2(x_{t,i,m}^{\text{Load,R}}) \leq (q+z) \\ 0 \leq z \leq T_1(x_{t,i,m}^{\text{Load,R}}), 0 \leq q \end{array} \right\} \tag{31b}$$

It can be observed that the reserve determination method for uncertain load power forecast error is consistent with that of RES. Therefore, for prosumers equipped with both RES and load, their reserve requirements can be determined after solving (5) and (31). Thus, the total upward/downward reserve requirements can be denoted as the right-hand side of (8c) and (8d), respectively.

The Monte Carlo simulation approach is used to generate 50000 scenarios of load power forecast error following the multivariate Gaussian distribution $\mathcal{N}(\mu^{\mathbf{d}}, \mathbf{\Sigma^d})$. The parameter settings of $\mathcal{N}(\mu^{\mathbf{d}}, \mathbf{\Sigma^d})$ are shown as follows:

$$\left\{ \begin{array}{l} \mathbf{\Sigma^d}_{i,i} = \zeta \sum_m P_{t,i,m}^{\text{Load}} \\ \mathbf{\Sigma^d}_{i,j} = \rho_{ij} \zeta \sum_r P_{t,i,m}^{\text{Load}} \sum_r P_{t,j,m}^{\text{Load}} \end{array} \right. \tag{32}$$

Note that we set $\mu^{\mathbf{d}} = \mathbf{0}$, $\zeta = 0.02$ and $\rho_{ij} = 0.01$ in all the simulations for the load uncertainty ambiguity formulation.

B. Considering the Uncertainty Associated with Upstream Electricity Price

The uncertainty of upstream electricity price $\pi_t^{\text{E,Grid}}$ is formulated within a box uncertainty set $\Theta_t^{\text{E,Grid}}$ as follows:

$$\Theta_t^{\text{E,Grid}} = \left\{ \pi_t^{\text{E,Grid}} : \pi_t^{\text{E,Grid}} = \widetilde{\pi}_t^{\text{E,Grid}} \pm \Delta\pi_t^{\text{E,Grid}} \kappa_t, \|\kappa_t\| \leq 1 \right\} \tag{33}$$

where $\widetilde{\pi}_t^{\text{E,Grid}}$ is the forecasted upstream electricity price and $\Delta\pi_t^{\text{E,Grid}}$ is the maximum deviation of $\pi_t^{\text{E,Grid}}$ compared with $\widetilde{\pi}_t^{\text{E,Grid}}$. κ_t is the deviation coefficient of $\pi_t^{\text{E,Grid}}$ compared with $\widetilde{\pi}_t^{\text{E,Grid}}$.

The uncertain part of the prosumer's operation cost function considering the uncertain $\pi_t^{\mathrm{E,Grid}}$ is formulated as:

$$\begin{aligned} C_{t,i}^{\mathrm{pro,uncertain}}(x_{t,i}^{\mathrm{pro}}) &= (\widetilde{\pi}_t^{\mathrm{E,Grid}} - \pi_t^{\mathrm{E,Grid}})P_{t,i}^{\mathrm{Grid}} + (\widetilde{\pi}_t^{\mathrm{E,P2P}} - \pi_t^{\mathrm{E,P2P}})E_{t,i} \\ &= (\widetilde{\pi}_t^{\mathrm{E,Grid}} - \pi_t^{\mathrm{E,Grid}})P_{t,i}^{\mathrm{Grid}} + \chi^{\mathrm{P2P}}(\widetilde{\pi}_t^{\mathrm{E,Grid}} - \pi_t^{\mathrm{E,Grid}})E_{t,i} \end{aligned} \tag{34}$$

where $C_{t,i}^{\mathrm{pro,uncertain}}(x_{t,i}^{\mathrm{pro}})$ denotes the uncertain part of the prosumer's operation cost considering the uncertainty of $\pi_t^{\mathrm{E,Grid}}$. χ^{P2P} is the P2P trading pricing coefficient of the adopted MMR pricing mechanism, i.e., $\widetilde{\pi}_t^{\mathrm{E,P2P}} = \chi^{\mathrm{P2P}}\widetilde{\pi}_t^{\mathrm{E,Grid}}, \pi_t^{\mathrm{E,P2P}} = \chi^{\mathrm{P2P}}\pi_t^{\mathrm{E,Grid}}$.

Therefore, by utilizing the RO approach to handle the uncertainty of $\pi_t^{\mathrm{E,Grid}}$, the objective function of the prosumer's operation cost can be reformulated as (35a) and the corresponding constraints are (35b)-(35e):

$$\min C_{t,i}^{\mathrm{pro,RO}}(x_{t,i}^{\mathrm{pro}}) \tag{35a}$$

$$C_{t,i}^{\mathrm{pro,RO}}(x_{t,i}^{\mathrm{pro}}) \geq C_{t,i}^{\mathrm{pro,certain}}(x_{t,i}^{\mathrm{pro}}) + C_{t,i}^{\mathrm{pro,uncertain}}(x_{t,i}^{\mathrm{pro}}) \tag{35b}$$

$$C_{t,i}^{\mathrm{pro,uncertain}}(x_{t,i}^{\mathrm{pro}}) = \max \left[\begin{array}{l} (\widetilde{\pi}_t^{\mathrm{E,Grid}} - \pi_t^{\mathrm{E,Grid}})P_{t,i}^{\mathrm{Grid}} \\ +\chi^{\mathrm{P2P}}(\widetilde{\pi}_t^{\mathrm{E,Grid}} - \pi_t^{\mathrm{E,Grid}})E_{t,i} \end{array} \right] \varpi_{t,i} \tag{35c}$$

$$0 \leq \varpi_{t,i} \leq 1 : \phi_{t,i} \tag{35d}$$

$$\left\{ \begin{array}{l} \textbf{RES Constraints: } (6a) - (6b). \\ \textbf{DG Constraints: } (7a) - (7e). \\ \textbf{Energy and Reserve Constraints:} \\ (8a) - (8f), (9a) - (9b). \\ \textbf{Carbon Constraints: } (13a) - (13e). \end{array} \right\} \tag{35e}$$

where $C_{t,i}^{\mathrm{pro,RO}}(x_{t,i}^{\mathrm{pro}})$ is the RO objective function of the prosumer's operation cost, $C_{t,i}^{\mathrm{pro,certain}}(x_{t,i}^{\mathrm{pro}})$ denotes the certain part of the prosumer's operation cost considering the uncertainty of $\pi_t^{\mathrm{E,Grid}}$. Note that $C_{t,i}^{\mathrm{pro,certain}}(x_{t,i}^{\mathrm{pro}})$ is consistent with $C_{t,i}^{\mathrm{pro}}(x_{t,i}^{\mathrm{pro}})$ in (15a). $\varpi_{t,i}$ is the conservative level variable ranging from 0 to 1 for considering the uncertainty of $\pi_t^{\mathrm{E,Grid}}$ and $\phi_{t,i}$ is the corresponding dual variable for (35d).

The dual problem of (35c)-(35d) can be formulated as follows:

$$\min \phi_{t,i} \tag{36a}$$

$$s.t. \left\{ \begin{array}{c} \phi_t \geq 0 \\ \phi_t \geq (\widetilde{\pi}_t^{\mathrm{E,Grid}} - \pi_t^{\mathrm{E,Grid}})(P_{t,i}^{\mathrm{Grid}} + \chi^{\mathrm{P2P}}E_{t,i}) \end{array} \right. \tag{36b}$$

By substituting (36) into (35), the RO problem of the prosumer can be rewritten as follows:

$$\min C_{t,i}^{\mathrm{pro,RO}}(x_{t,i}^{\mathrm{pro}}) = C_{t,i}^{\mathrm{pro,certain}}(x_{t,i}^{\mathrm{pro}}) + \phi_{t,i} \tag{37a}$$

$$s.t. \left\{ \begin{array}{l} \textbf{RES Constraints: } (6a) - (6b). \\ \textbf{DG Constraints: } (7a) - (7e). \\ \textbf{Energy and Reserve Constraints:} \\ (8a) - (8f), (9a) - (9b). \\ \textbf{Carbon Constraints: } (13a) - (13e). \\ \textbf{Dual Constraints for RO: } (36b). \end{array} \right\} \tag{37b}$$

Therefore, the reformulated RO model for prosumer is still a convex optimization problem like (15) and can be solved efficiently by off-the-shelf commercial solvers like Gurobi.

REFERENCES

[1] F. Egli, B. Steffen, and T. S. Schmidt, "A dynamic analysis of financing conditions for renewable energy technologies," *Nature Energy*, vol. 3, no. 12, pp. 1084–1092, 2018.

[2] M. Mishra, A. Singh, R. K. Misra, and D. Singh, "Peer-to-peer energy trading with active participation of distributed generation," *IEEE Internet of Things Journal*, vol. 10, no. 23, pp. 21 076–21 088, 2023.

[3] Y. Wang, C.-F. Chen, P.-Y. Kong, H. Li, and Q. Wen, "A Cyber–Physical–Social Perspective on Future Smart Distribution Systems," *Proceedings of the IEEE*, vol. 111, no. 7, pp. 694–724, 2023.

[4] F. Si, N. Zhang, Y. Wang, P.-Y. Kong, and W. Qiao, "Distributed optimization for integrated energy systems with secure multiparty computation," *IEEE Internet of Things Journal*, vol. 10, no. 9, pp. 7655–7666, 2022.

[5] O. Jogunola, Y. Tsado, B. Adebisi, and M. Hammoudeh, "Virtelect: A peer-to-peer trading platform for local energy transactions," *IEEE Internet of Things Journal*, vol. 9, no. 8, pp. 6121–6133, 2021.

[6] Z. Li, L. Wu, Y. Xu, L. Wang, and N. Yang, "Distributed tri-layer risk-averse stochastic game approach for energy trading among multi-energy microgrids," *Applied Energy*, vol. 331, p. 120282, 2023.

[7] E. Sorin, L. Bobo, and P. Pinson, "Consensus-based approach to peer-to-peer electricity markets with product differentiation," *IEEE Transactions on Power Systems*, vol. 34, no. 2, pp. 994–1004, 2018.

[8] A. Forestiero and G. Papuzzo, "Agents-based algorithm for a distributed information system in internet of things," *IEEE Internet of Things Journal*, vol. 8, no. 22, pp. 16 548–16 558, 2021.

[9] C. Zhou, C. Feng, and Y. Wang, "Spatial–Temporal Energy Management of Base Stations in Cellular Networks," *IEEE Internet of Things Journal*, vol. 9, no. 13, pp. 10 588–10 599, 2022.

[10] T. Morstyn, N. Farrell, S. J. Darby, and M. D. McCulloch, "Using peer-to-peer energy-trading platforms to incentivize prosumers to form federated power plants," *Nature Energy*, vol. 3, no. 2, pp. 94–101, 2018.

[11] X. Chang, Y. Xu, Q. Guo, H. Sun, and W. K. Chan, "A byzantine-resilient distributed peer-to-peer energy management approach," *IEEE Transactions on Smart Grid*, vol. 14, no. 1, pp. 623–634, 2022.

[12] M. H. Ullah and J.-D. Park, "Peer-to-peer energy trading in transactive markets considering physical network constraints," *IEEE Transactions on Smart Grid*, vol. 12, no. 4, pp. 3390–3403, 2021.

[13] X. Wei, J. Liu, Y. Xu, and H. Sun, "Virtual power plants peer-to-peer energy trading in unbalanced distribution networks: A distributed robust approach against communication failures," *IEEE Transactions on Smart Grid*, pp. 1–1, 2023.

[14] T. Morstyn and M. D. McCulloch, "Multiclass energy management for peer-to-peer energy trading driven by prosumer preferences," *IEEE Transactions on Power Systems*, vol. 34, no. 5, pp. 4005–4014, 2018.

[15] K. Zhang, S. Troitzsch, S. Hanif, and T. Hamacher, "Coordinated market design for peer-to-peer energy trade and ancillary services in distribution grids," *IEEE Transactions on Smart Grid*, vol. 11, no. 4, pp. 2929–2941, 2020.

[16] L. Wang, Z. Wang, Z. Li, M. Yang, and X. Cheng, "Distributed optimization for network-constrained peer-to-peer energy trading among multiple microgrids under uncertainty," *International Journal of Electrical Power & Energy Systems*, vol. 149, p. 109065, 2023.

[17] X. Li, C. Li, X. Liu, G. Chen, and Z. Y. Dong, "Two-Stage Community Energy Trading Under End-Edge-Cloud Orchestration," *IEEE Internet of Things Journal*, vol. 10, no. 3, pp. 1961–1972, 2023.

[18] Z. Chen, Z. Li, C. Guo, J. Wang, and Y. Ding, "Fully Distributed Robust Reserve Scheduling for Coupled Transmission and Distribution Systems," *IEEE Transactions on Power Systems*, vol. 36, no. 1, pp. 169–182, 2021.

[19] M. Vahedipour-Dahraie, H. Rashidizadeh-Kermani, M. Shafie-Khah, and P. Siano, "Peer-to-peer energy trading between wind power producer and demand response aggregators for scheduling joint energy and reserve," *IEEE Systems Journal*, vol. 15, no. 1, pp. 705–714, 2020.

[20] Z. Guo, P. Pinson, S. Chen, Q. Yang, and Z. Yang, "Chance-constrained peer-to-peer joint energy and reserve market considering renewable generation uncertainty," *IEEE Transactions on Smart Grid*, vol. 12, no. 1, pp. 798–809, 2020.

[21] J. Li, M. E. Khodayar, J. Wang, and B. Zhou, "Data-driven distributionally robust co-optimization of p2p energy trading and network operation for interconnected microgrids," *IEEE Transactions on Smart Grid*, vol. 12, no. 6, pp. 5172–5184, 2021.

[22] W. Liu, Y. Xu, J. Liu, W. Yin, Y. Hou, and Z. Yang, "Energy and reserve sharing considering uncertainty and communication resources," *IEEE Internet of Things Journal*, vol. 10, no. 14, pp. 12 627–12 637, 2023.

[23] Y. Wang, J. Qiu, Y. Tao, and J. Zhao, "Carbon-oriented operational planning in coupled electricity and emission trading markets," *IEEE Transactions on Power Systems*, vol. 35, no. 4, pp. 3145–3157, 2020.

[24] Z. Lu, L. Bai, J. Wang, J. Wei, Y. Xiao, and Y. Chen, "Peer-to-peer joint electricity and carbon trading based on carbon-aware distribution locational marginal pricing," *IEEE Transactions on Power Systems*, vol. 38, no. 1, pp. 835–852, 2022.

[25] T. Wan, Y. Tao, J. Qiu, and S. Lai, "Distributed energy and carbon emission right trading in local energy systems considering the emission obligation on demand side," *IEEE Systems Journal*, vol. 17, no. 4, pp. 6292–6301, 2023.

[26] H. Yao, Y. Xiang, C. Gu, and J. Liu, "Peer-to-peer coupled trading of energy and carbon emission allowance: A stochastic game-theoretic approach," *IEEE Internet of Things Journal*, pp. 1–1, 2023.

[27] R. Xin and U. A. Khan, "Distributed heavy-ball: A generalization and acceleration of first-order methods with gradient tracking," *IEEE Transactions on Automatic Control*, vol. 65, no. 6, pp. 2627–2633, 2019.

[28] J.-F. Aujol, C. Dossal, and A. Rondepierre, "Optimal convergence rates for nesterov acceleration," *SIAM Journal on Optimization*, vol. 29, no. 4, pp. 3131–3153, 2019.

[29] L. Yang, Y. Xu, H. Sun, and W. Wu, "Tractable convex approximations for distributionally robust joint chance-constrained optimal power flow under uncertainty," *IEEE Transactions on Power Systems*, vol. 37, no. 3, pp. 1927–1941, 2021.

[30] M. Elkin, "Distributed exact shortest paths in sublinear time," *Journal of the ACM (JACM)*, vol. 67, no. 3, pp. 1–36, 2020.

[31] W. Tushar, T. K. Saha, C. Yuen, T. Morstyn, M. D. McCulloch, H. V. Poor, and K. L. Wood, "A motivational game-theoretic approach for peer-to-peer energy trading in the smart grid," *Applied Energy*, vol. 243, pp. 10–20, 2019.

[32] Li, Jing and Ye, Yujian and Papadaskalopoulos, Dimitrios and Strbac, Goran, "Computationally Efficient Pricing and Benefit Distribution Mechanisms for Incentivizing Stable Peer-to-Peer Energy Trading," *IEEE Internet of Things Journal*, vol. 8, no. 2, pp. 734–749, 2021.

[33] C. Mu, T. Ding, S. Zhu, O. Han, P. Du, F. Li, and P. Siano, "A Decentralized Market Model for a Microgrid With Carbon Emission Rights," *IEEE Transactions on Smart Grid*, vol. 14, no. 2, pp. 1388–1402, 2023.

[34] Y. Wu, T. Zhao, H. Yan, M. Liu, and N. Liu, "Hierarchical Hybrid Multi-Agent Deep Reinforcement Learning for Peer-to-Peer Energy Trading Among Multiple Heterogeneous Microgrids," *IEEE Transactions on Smart Grid*, vol. 14, no. 6, pp. 4649–4665, 2023.

[35] S. Boyd, N. Parikh, E. Chu, B. Peleato, J. Eckstein *et al.*, "Distributed optimization and statistical learning via the alternating direction method of multipliers," *Foundations and Trends® in Machine learning*, vol. 3, no. 1, pp. 1–122, 2011.

[36] A. Buccini, P. Dell'Acqua, and M. Donatelli, "A general framework for admm acceleration," *Numerical Algorithms*, vol. 85, pp. 829–848, 2020.

[37] X. Yang, Z. Song, J. Wen, L. Ding, M. Zhang, Q. Wu, and S. Cheng, "Network-constrained transactive control for multi-microgrids-based distribution networks with soft open points," *IEEE Transactions on Sustainable Energy*, vol. 14, no. 3, pp. 1769–1783, 2023.

[38] Z. Song, "Data sheet for the carbon-aware p2p joint energy and reserve trading market," https://github.com/szh16886596/Data-sheet-for-P2P-Trading-Market.git.

[39] H. Wang, Z. Bie, and H. Ye, "Locational Marginal Pricing for Flexibility and Uncertainty With Moment Information," *IEEE Transactions on Power Systems*, vol. 38, no. 3, pp. 2761–2775, 2023.

[40] H. Ghasemnejad, M. Rashidinejad, A. Abdollahi, and S. Dorahaki, "Energy management in citizen energy communities: A flexibility-constrained robust optimization approach considering prosumers comfort," *Applied Energy*, vol. 356, p. 122456, 2024.

Zehao Song received the B.S. degree in electrical engineering from the Zhejiang University of Technology in 2022. He is now pursuing the M.S. degree in electrical engineering at Tsinghua Berkeley Shenzhen Institute (TBSI), Tsinghua Shenzhen International Graduate School (SIGS), Tsinghua University. His research interest includes energy management of power systems and distributed optimization.

Yinliang Xu (Senior Member, IEEE) received the B.S. and M.S. degrees in control science and engineering from the Harbin Institute of Technology, Harbin, China, in 2007 and 2009, respectively, and the Ph.D. degree in electrical and computer engineering from New Mexico State University, Las Cruces, NM, USA, in 2013. He is currently an Associate Professor with Tsinghua-Berkeley Shenzhen Institute (TBSI), Tsinghua Shenzhen International Graduate School (SIGS), Tsinghua University, China. His research interests include distributed control and optimization of power systems, and renewable energy integration. He is an Associate Editor for the *IET Renewable Power Generation*, *IET Smart Grid*, and *IET Generation, Transmission & Distribution*.

Lun Yang received the Ph.D. degree in Electrical Engineering from Tsinghua University, Beijing, China, in 2022. He is currently an Assistant Professor in the School of Automation Science and Engineering of Xi'an Jiaotong University. Before that, he was a visiting scholar with The Chinese University of Hong Kong, Shenzhen, from October 2022 to April 2023. His research interests include power and energy systems operations and data-driven optimization under uncertainty. He was the recipient of the best paper award at 2020 IEEE PES General Meeting.

Hongbin Sun (Fellow, IEEE) received the double B.S. degrees from Tsinghua University, Beijing, China, in 1992, and the Ph.D. degree from the Department of Electrical Engineering, Tsinghua University, in 1996. From September, 2007 to September, 2008, he was a Visiting Professor with the School of EECS, the Washington State University, Pullman, USA. He is currently the ChangJiang Scholar Chair Professor with the Department of Electrical Engineering and the Director of energy management and control research center, Tsinghua University. His technical research interests area include electric power system operation and control with specific interests on the energy management system, system-wide automatic voltage control, and energy system integration.